A NOVEL ROLE FOR ODORANT BINDING PROTEINS IN DEACTIVATION OF *DROSOPHILA* OLFACTORY NEURONS

APPROVED BY SUPERVISORY COMMITTEE

Dean Smith, MD, PhD

Julian Meeks, PhD

Helmut Kramer, PhD

Jonathan Terman, PhD

A NOVEL ROLE FOR ODORANT BINDING PROTEINS IN DEACTIVATION OF *DROSOPHILA* OLFACTORY NEURONS

by

ELIZABETH ANNE SCHEUERMANN

DISSERTATION / THESIS

Presented to the Faculty of the Graduate School of Biomedical Sciences

The University of Texas Southwestern Medical Center at Dallas

In Partial Fulfillment of the Requirements

For the Degree of

DOCTOR OF PHILOSOPHY

The University of Texas Southwestern Medical Center at Dallas

Dallas, Texas

August, 2019

Copyright

by

Elizabeth Anne Scheuermann, 2019

All Rights Reserved

DEDICATION

I would like to thank Dean for his patience and mentorship. I would also like to thank my wonderful husband Alex for all the support he provided and the many discussions we had about my work. Thank you to my family for nurturing my love of science and for your support through these many years of education. And thank you to the many friends I've made along the way.

Publication No._____

Elizabeth Anne Scheuermann

The University of Texas Southwestern Medical Center at Dallas, Graduation Year

Supervising Professor: Dean Perry Smith, MD, PhD

In insects, odorant binding proteins are a large and diverse group of low molecular weight proteins secreted into the fluid bathing olfactory and gustatory dendrites. The best-characterized OBP, known as LUSH, is required in *Drosophila* melanogaster for the detection of physiological levels of the male-specific pheromone cVA. While LUSH acts as a sensitizing factor for pheromone detection, the role of other OBPs encoded in the *Drosophila* genome is largely unknown. In an effort to characterize members of this family, I used CRISPR-Cas9 to generate and characterize a deletion of two genes encoding the homologous OBPs *OS-E* and *OS-F*. These OBPs are nearly 70% identical and their expression is restricted to a small set of antennal chemosensory sensilla. Electrophysiological analysis of the olfactory neurons within these sensilla revealed no major difference in odorant sensitivity or specificity in the mutants but did reveal a striking deactivation defect to a subset of odorants. Surprisingly, other odorants detected

by the same receptor are differentially affected by the absence of *OS-E* and *OS-F*, revealing an odorant-specific role for these OBPs in deactivation kinetics. Activation kinetics remain normal for the affected odorants in mutants. Genomic rescue experiments revealed that *OS-E* and *OS-F* are also functionally redundant, as either OBP is sufficient to revert the mutant phenotype. My findings reveal a new role for OBPs in deactivation of olfactory neurons and expand our understanding of the range of OBP functions.

TABLE OF CONTENTS

ABSTRACT iv

PRIOR PUBLICATIONS vii

CHAPTER ONE INTRODUCTION 1

CHAPTER TWO REVIEW OF THE LITERATURE 3

CHAPTER THREE MATERIALS AND METHODS 37

CHAPTER FOUR RESULTS 47

CHAPTER FIVE CONCLUSIONS AND RECOMMENDATIONS 64

SUMMARY 67

BIBLIOGRAPHY 74

PRIOR PUBLICATIONS

Pitts S, Pelser E, Meeks J, Smith D. Odorant Responses and Courtship Behaviors Influenced by at4 Neurons in Drosophila. PLoS One. 2016;11(9):e0162761. doi: 10.1371/journal.pone.0162761. PubMed PMID: 27617442; PMCID: PMC5019410

Scheuermann E, Smith D. Odor-specific deactivation defects in an odorant binding protein mutant. Genetics. In revision. 2019.

Park A, Tran T, Scheuermann E, Gutierrez L, Stojanik C, Plyler J, Thompson G, Smith D, Atkinson N. Alcohol Increases Aggression in Flies. eLife. In revision. 2019.

LIST OF FIGURES

FIGURE 2-1. INTERNAL ORGANIZATION OF A *DROSOPHILA* OLFACTORY SENSILLUM 4

FIGURE 2-2. A MODEL FOR CVA SENSING AND THE ROLE OF LUSH 24

FIGURE 2-3. PROPOSED MODELS FOR THE FUNCTION OF *DROSOPHILA* OBPS OBP49A AND OBP28A..... 31

FIGURE 3-1. GENERATION OF AN *OS-E/F* MUTANT 39

FIGURE 4-1. SPONTANEOUS AND EVOKED ACTIVITY FROM WILD TYPE AND *OS-E/F* MUTANTS 49

FIGURE 4-2. DEACTIVATION KINETICS ARE ABNORMAL TO A SUBSET OF ODORANTS IN *OS-E/F* MUTANTS 51

FIGURE 4-3. ODORANT SPECIFICITY OF THE OR83C DEACTIVATION DEFECT 54

FIGURE 4-4. ACTIVATION KINETICS FOR FARNESOL AND CVA ARE NOT AFFECTED BY LOSS OF *OS-E* AND *OS-F* 56

FIGURE 4-5. PEAK ACTIVATION IN *OS-E/F* MUTANTS 59

FIGURE 4-6. *OS-E/F* MUTANTS SHOW A STRONGER DEACTIVATION DEFECT THAN SNMP MUTANTS 61

FIGURE 4-7. *OS-E* AND *OS-F* ARE FUNCTIONALLY REDUNDANT FOR RAPID NEURONAL DEACTIVATION 63

FIGURE 5-1. A PROPOSED MODEL FOR *OS-E/F* FUNCTION IN DEACTIVATION 68

LIST OF TABLES

TABLE 2-1. OLFACTORY SENSILLA OF THE ANTENNAE, IDENTITY OF THE OSNS, AND BEST KNOWN LIGANDS 33

TABLE 2-2. *DROSOPHILA* OBPS AND THEIR EXPRESSION IN ADULT CHEMOSENSORY ORGANS 35

LIST OF APPENDICES

APPENDIX A. EXPRESSION OF MYC-TAGGED *OS-E* 69

APPENDIX B. RTPCR VERIFICATION OF *OS-E/F* MUTANT 70

APPENDIX C. ELECTROPHYSIOLOGY DATA AND STATISTICS..... 71

LIST OF DEFINITIONS

ab – antennal basiconic

ac – antennal coeloconic

ai – antennal intermediate

at – antennal trichoid

cVA – 11-cis vaccenyl acetate

Gr – gustatory receptor

Ir – ionotropic receptor

OBP – odorant binding protein

Or – odorant receptor

Orco – odorant receptor coreceptor (Or83b)

OSN – olfactory sensory neuron

PBP – pheromone binding protein

Spikes/s – spikes per second

SSR – single sensillum recording

CHAPTER ONE
Introduction

The insect olfactory system has a significant impact on human health. The mosquito species *Anopheles gambiae* and *Aedes aegypti* feed on human blood and thereby spread diseases including malaria, West Nile, and dengue. Females identify potential sources of food through olfactory cues including exhaled carbon dioxide and human body odors[1, 2]. The use of neurotoxic pesticides, while effective against mosquitos, has also profoundly impacted both human populations and non-target beneficial insects such as honeybees[3, 4]. One alternative to the use of neurotoxins is manipulation of the olfactory system[5]. This could impact the ability of pest insects to find host targets or mates. Identifying potential targets for species-specific nontoxic pest control therefore requires a detailed understanding of the olfactory systems of insects.

Drosophila melanogaster provides an especially attractive model for the insect olfactory system owing to its rapid generation time and well-characterized genome. Additionally, there are a number of genetic tools available for precisely dissecting the function of individual genes and proteins. The tuning of individual *Drosophila* olfactory neurons has largely been characterized through a combination of electrophysiological and behavioral assays. These efforts have recently offered insight into the mechanism by which DEET acts as an effective mosquito repellant, expanding our knowledge of how the insect olfactory system can be manipulated for effective pest control[6, 7].

Although the tuning of individual olfactory neurons is well understood, many questions remain about the mechanisms of odorant signal transduction. The olfactory systems of virtually all insect species contain a number of soluble non-neuronal proteins—odorant binding

proteins— whose precise function is not well defined. These proteins are essential for pheromone sensing in many insect species, including *Drosophila*[8-11]. However, many of these proteins remain uncharacterized even in *Drosophila*. I am interested in identifying roles for odorant binding proteins in olfaction.

I have generated a novel mutant in which two related odorant binding protein genes, OS-E and OS-F, are missing. Through electrophysiology I have determined that these two proteins are important for the rapid deactivation of a subset of olfactory neurons to their respective ligands. This represents a novel role for odorant binding proteins in the termination of odorant responses rather than odorant sensitivity and expands our understanding of how these proteins function in the insect olfactory system.

CHAPTER TWO
Review of the Literature

ANATOMY OF THE *DROSOPHILA* OLFACTORY SYSTEM

Olfactory organs of *Drosophila* melanogaster

The olfactory organs of *Drosophila* consist of antennae and maxillary palps that are both found on the head[12]. As in vertebrates, the olfactory system consists of olfactory sensory neurons (OSNs) and auxiliary cells (also called support cells) in an aqueous environment[12]. The insect olfactory system is highly compartmentalized, with OSNs housed in hair-like structures called sensilla[12]. The interior of a sensillum is hollow and houses the dendrites of one to four OSNs that are studded with receptors conferring the tuning of each OSN (**Figure 2-1**)[13]. Each dendrite in a sensillum typically expresses only a single class of receptor. The dendrites are bathed in aqueous sensillum lymph that is secreted by the non-neuronal support cells[13]. The cuticle of the sensillum is perforated by a number of pores that facilitate the entry of odorant molecules into the sensillum lymph[14]. Molecules can then pass through the lymph and bind the receptors on the dendrites of OSNs, activating the neuron. We measure the response of OSNs to odorants in vivo using single sensillum recordings (SSR). In brief, a glass reference electrode filled with artificial sensillum lymph is placed in the eye, and a recording electrode pierces through the cuticle of an individual sensillum without contacting the dendrites[11, 15]. The activity of all neurons present in a sensillum is shown as spikes of varying amplitude and frequency, with spikes increasing in frequency if one of the neurons is

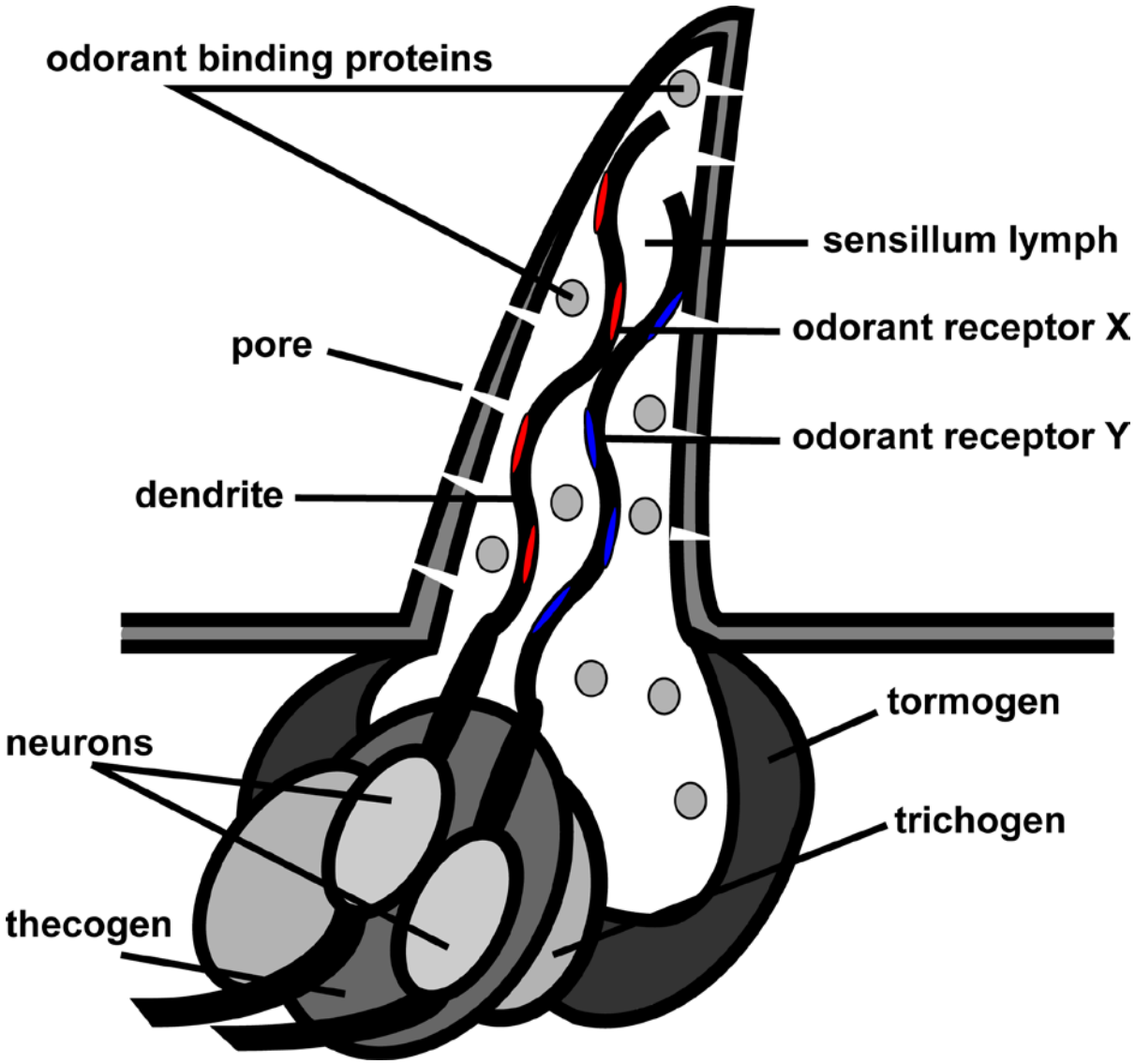

Figure 2-1. Internal organization of a *Drosophila* olfactory sensillum. Cartoon cross-section of a generic olfactory sensillum housing the dendrites of two olfactory neurons. Each neuron expresses a unique odorant receptor gene. Dendrites are bathed in sensillum lymph secreted by the non-neuronal support cells. Sensillum lymph contains OBPs secreted by support cells. Odorant molecules pass through pores in the cuticle of the sensillum and move through the sensillum lymph to the receptors on the dendrites.

tuned to an odorant passed across the preparation[15]. Sensilla are classified by their morphology and the range of odors detected by neurons in each morphological class (Table 2-1)[12]. All four classes are found on the third segment of the antenna (funiculus), while the maxillary palps only have one class.

Basiconic sensilla

Basiconic sensilla can be further subdivided based on their length and thickness into large (~12µm long), small (~9µm long), and thin (~12µm long but more slender than large) basiconics[12]. Large basiconic sensilla are found exclusively at the base of the funiculus[12]. Other basiconic sensilla are found across all surfaces of the funiculus excepting the dorso-lateral region occupied primarily by trichoid sensilla[12]. Basiconic sensilla are also the only sensillum class found on the maxillary palp. The cuticular walls of basiconic sensilla are relatively thin, 100-130nm, with a few small basiconics having walls as thick as 200nm[12]. The pores that perforate the cuticular walls are arranged in longitudinal walls down the length of the hair[12]. Interestingly, the dendrites of each OSN in a basiconic sensillum show substantial branching at the distal end, such that a “bush-like” structure is observed in cross-sections[12].

Each basiconic sensillum houses the dendrites of two to four OSNs that each typically express one or two *Odorant receptor* (*Or*) genes[16]. The basiconic sensilla can therefore be classified not only by their morphology but by the identities of specific odorant receptor genes expressed in each subtype. There are a total of ten basiconic sensilla[16, 17]. The OSNs of basiconic sensilla are tuned to broad ranges of odorants found in typical fly food sources, with overlapping

sensitivity between different odorant receptors[15-17]. One exception is the ab1c neuron that expresses gustatory receptors tuned specifically to CO_2, which is discussed later in this review[18].

The ab3 sensillum in particular has been a valuable resource in the study of individual *Drosophila Or* genes. An "empty neuron" system was devised by generating flies lacking the OR22a receptor normally found in ab3 sensilla, and using the *Or22a* promoter to drive expression of the *Or* gene of interest[19]. This system was used to broadly characterize the tuning of the *Drosophila Or* gene family, as the majority of *Ors* are found in basiconic sensilla[16]. However it is worth noting that this approach has not been successful in characterizing the endogenous tuning of *Ors* expressed in non-basiconic sensilla[20].

Trichoid sensilla

Trichoid sensilla are distributed on the dorso-lateral region of the funiculus[12]. They are the longest sensilla on the antennae, ranging from 18-22µm in length[12]. The cuticle wall of trichoid sensilla is also the thickest, 350-450nm, though the thickness decreases as the sensillum tapers towards its tip. Unlike other sensilla, trichoid sensilla possess a thick cylindrical base referred to as the "basal drum." There are significantly fewer pores in the cuticle walls of trichoid sensilla, relative to other sensillum classes, and their distribution is irregular. Unlike basiconic sensilla, the dendrites of trichoid sensilla do not exhibit much branching. Trichoid sensilla are known to house pheromone-sensing OSNs in other insect species, and this is generally true of *Drosophila* as well[21].

There are two classes of trichoid sensilla in *Drosophila* that house one or three OSNs respectively and are referred to as at1 and at4[16, 22]. Expression of trichoid-specific *Or* genes in

the “empty basiconic” preparation failed to demonstrate the endogenous tuning of these receptors. This is partly due to the absence of neuronal and non-neuronal factors discussed later in the text. The neuron in the at1 sensillum expresses the *Or* gene *Or67d* that exclusively senses the male-specific pheromone 11-*cis* vaccenyl acetate (cVA)[23]. Two of the OSNs in the at4 sensillum express a single class of odorant receptors, either Or47b or Or88a[16]. Recent work identified the fly pheromone methyl laurate as the exclusive ligand of Or47b, while Or88a was activated exclusively by methyl myristate and methyl palmitate[24]. However, an extensive odorant screen revealed that both of these neurons are tuned to a wide range of both food and fly odors, refuting the notion that they are dedicated sensors of other fly compounds[25]. The third neuron in at4 sensilla expresses three closely-related odorant receptors: Or65a, Or65b, and Or65c. Or65a was identified as a cVA sensor using the “empty basiconic” preparation[26]. This assay demonstrated that direct application of liquid cVA to the sensillum activated the Or65a-expressing neuron. However, liquid cVA application does not activate the Or65abc neuron in the endogenous trichoid sensillum. To date, no strong ligand has been identified for the Or65abc neuron, though optogenetic activation of the neuron during courtship suppresses courtship behavior and mating success[25].

Intermediate sensilla

Intermediate sensilla are named for their structure, which is intermediate to that of basiconic and trichoid sensilla[12]. Their morphology is broadly similar to that of trichoid sensilla, excepting the shorter length (12-15µm) and the substantial dendritic branching associated with basiconic dendrites[12]. Intermediate sensilla are distributed along the same regions as trichoids[12].

Two classes of intermediate sensilla were originally identified, housing the dendrites of two or three OSNs. Later work conflated the intermediate sensilla with trichoid, naming them as at2 and at3 respectively. A recent study re-established the division of intermediate and trichoid sensilla based on morphological features, and identified a third intermediate sensillum that is innervated by one OSN (ai1)[22]. Two neurons located in intermediate sensilla express *Or* genes that have had their tuning thoroughly characterized in their endogenous sensilla—Or83c and Or19a. Or83c is a narrowly tuned sensor of the citrus peel compound farnesol that acts as an attractant and possible oviposition cue[20]. Or19a is tuned to several citrus peel compounds, but most strongly to limonene that is not attractive but specifically triggers oviposition[27].

Coeloconic sensilla

Coeloconic sensilla comprise the shortest class of sensilla in *Drosophila* with an average length of 5µm[12]. Unlike all other olfactory sensilla, coeloconic sensilla possess a double-walled cuticle[12]. The outer wall is 110nm thick while the inner wall is 30nm thick. Instead of pores, the outer cuticle forms approximately eight cuticular fingers with grooved channels running the length of the hair[12]. The dendrites are also surrounded with a dendrite sheath not seen in basiconic or trichoid sensilla[12]. Coeloconic sensilla are irregularly distributed across the funiculus, with one small cluster occurring close to the arista[12]. They are also found in the sacculus, a three-chambered pit in the antenna that senses environmental humidity[28].

There are four classes of coeloconic sensilla that house the dendrites of one to three OSNs. While the majority of trichoid and basiconic dendrites express Or genes, the dendrites of coeloconic sensilla express Ionotropic receptor (Ir) genes that are reviewed later in the text[29].

The one exception is an ac3 neuron that expresses one *Ir* and one *Or*. Coeloconic OSNs are tuned to acids, aldehydes, and ammonia[30, 31].

Support cells

Each sensillum is formed and maintained by a group of non-neuronal support cells[13]. The tormogen (socket) cell is the only support cell to directly contact the cuticle, and forms a complete sheath around the sensillum lymph cavity[13]. The trichogen (shaft) cell forms a more internal sheath around another support cell and the dendrites of OSNs. The thecogen (sheath) cell forms a "sleeve" around the outer dendritic segment at the base of the sensillum[13]. Coeloconic sensilla possess an outer an inner tormogen cell, and have a conspicuous dendrite sheath surrounding the outer dendritic segments[13]. This sheath merges with the inner cuticular wall at the distal end, causing the coeloconic sensillum to be split into two discrete inner and outer sensillum lymph cavities[13].

Receptors of the *Drosophila* olfactory system

Odorant receptors

Odorant receptor genes comprise the largest gene family in the *Drosophila* genome, with 62 members[32-34]. The first *Drosophila* Or genes were identified following Buck's 1991 discovery that vertebrate *Or* genes are 7 transmembrane domain G-coupled protein receptors[35]. Insect *Ors* were predicted to be GPCRs based on several pieces of evidence: 1) stimulation of antennal preparations with odorant or pheromone resulted in a rapid transient increase in inositol 1,4,5-

triphosphate (IP3), a component of the G protein signaling cascade, and 2) *norpA* mutants lacking phospholipase C (PLC), another component of G protein signaling, show decreased odorant responses in the maxillary palp[36-38]. In 1999 Clyne *et al*. searched the annotated *Drosophila* genome (then 10% complete) to identify potential *Or* genes[32]. Candidate genes were identified using an algorithm that searched the genome for potential open reading frames (ORFs) and refined the results by screening for putative proteins with multiple membrane-spanning domains. RT-PCR and RNA *in situ* hybridization were then used to determine if the expression of candidate receptors was restricted to the olfactory organs. This set of experiments identified the first *Or* genes in *Drosophila*, and demonstrated that *Drosophila* odorant receptors encode 7 transmembrane domains, similar to GPCRs. Gao *et al*. and Vosshall *et al*. published similar results identifying 100-200 putative *Or* genes in the *Drosophila* genome[33, 34].

The *Or* genes of *Drosophila* and other insects share little homology with those found in vertebrates. In 2006 Benton *et al*. identified the reason for this apparent discrepancy: the topology of insect Or proteins is inverted compared to that of vertebrate Ors[39]. Where classical vertebrate GPCRs, including vertebrate odorant receptors, have an intracellular C-terminus and an extracellular N-terminus, the insect C-terminus is extracellular and the N-terminus intracellular[39, 40]. This flipped orientation was verified in multiple Ors by fusing β-gal to the N or C-terminus of the *Or* and expressing the construct in a *Drosophila* cell line, followed by X-gal staining. Since β-gal is enzymatically active only in the cytosol, X-gal staining reveals whether each terminus is intracellular or extracellular. Indeed, X-gal staining was only observed when β-gal was fused to the N-terminus. The functional implications of this reversed topology, and its role in odorant signal transduction, are discussed later in the chapter.

Orco

Or genes are expressed exclusively in the neurons of trichoid, intermediate, and basiconic sensilla, with one receptor also found in a coeloconic sensillum[16]. Generally the expression of each Or is restricted such that an Or is only found in one neuron of a sensillum[16]. However, *Or83b* is broadly expressed across multiple sensillum types and in multiple neurons of a given sensillum[41]. Mapping of *Or83b* expression shows that it is always co-expressed with other Ors[41]. Expression of Or83b in an OSN without another Or results in a neuron with no odor sensitivity. Conversely, in *Or83b* null mutants the "tuning" OR protein is localized only to the cell body instead of at the dendrites, suggesting that Or83b is essential for normal trafficking of OR proteins. These neurons are also completely odor insensitive, as demonstrated through electrophysiology and olfactory behavior assays[41]. Deletion of the tuning receptor in a neuron in which Or83b is still expressed eliminates odorant sensitivity[42]. However, Orco alone can form functional odorant-gated ion channels that are activated by VUAA1[43]. *Or83b* is therefore also known as the *Odorant receptor coreceptor*, or *Orco*.

Orco is highly conserved across insect species, with some homologs sharing 70% amino acid identity with that of *Drosophila melanogaster*[44]. Trafficking of *Drosophila* Ors and odorant sensitivity are restored when *Orco* homologs from other insects are transgenically expressed in *Orco* mutants[45]. Recently cryo-EM has been used to resolve the crystal structure of Orco from the parasitic fig wasp *Apocrypta bakeri*[46]. An Orco homotetramer forms a "pinwheel" where four subunits circle a central pore which is thought to act as an ion channel. When expressed in mammalian cells, the Orco homotetramer acts as an ion channel, something previously observed

in other heterologous expression experiments[43, 47]. Butterwick *et al*. then mutated a set of conserved residues that contribute to the formation of the pore channel and showed that mutating these residues to alanine drastically reduced the sensitivity of the Orco complex to the ligand VUAA1. However, when an *Orco* mutant was co-expressed with an Or, the cell regained functional sensitivity to the known ligand of that Or. It is therefore likely that Orco and Ors form heteromeric complexes where both Orco and the Or form the pore channel[46, 48].

The Smith lab has also demonstrated that Orco is critical for the desensitization of Ors to their respective ligands[49]. The serine residue at position 289 is phosphorylated when the neuron is not activated by an odorant[49]. Prolonged exposure to an odorant, leading to prolonged activation of the neuron, eventually results in dephosphorylation of serine 289, reducing the sensitivity of the odorant receptor complex[49]. Replacing Ser289 with alanine generates an "inert" form of Orco that, when expressed in the fly, shows constitutively reduced sensitivity to odorants regardless of previous odor exposure[49]. Conversely, replacing Ser289 with aspartate mimics the phosphorylated state and increases sensitivity of the receptor complex to its ligand[49]. Orco therefore acts as a molecular "switch" regulating the sensitivity of Ors to their ligands.

Gustatory receptors

Gustatory receptors (Grs), like Ors, are 7TM receptors with an inverted topology respective to vertebrate Ors. The *Gr* family was initially distinguished from the *Or* family by characterizing their expression which revealed a subset of putative chemoreceptors expressed exclusively in the proboscis[50]. A screen for other putative members of the *Gr* family revealed two Grs expressed exclusively in the *Drosophila* antennae[51]. Gr21a and Gr63a are co-expressed

exclusively in a neuron in the ab1 sensillum[52]. This neuron is essential for detection of CO_2, which is a major component of *Drosophila* stress odorant[18]. Either gene alone is not sufficient to confer CO_2 sensitivity, suggesting that these receptors heterodimerize[53]. This complex does not require *Orco* expression, consistent with the rule that *Orco* is not found in OSNs that do not express *Or* genes.

Ionotropic receptors

Ionotropic receptors (Irs) were identified in a large-scale bioinformatics screen to find insect-specific orthologous genes in the *Drosophila* genome[29]. Six of the genes encoded proteins annotated as ionotropic glutamate receptors, and later searches of the *Drosophila* genome identified 66 Ir genes and 9 putative pseudogenes[29]. Unlike other Drosophila olfactory receptors, Irs are comprised of 3 transmembrane domains[29]. Although Ir genes have a similar molecular organization to canonical glutamate receptors, phylogenetic analysis shows no close relation between the two families.

Of the 66 *Ir* genes, only 17 are expressed on the antennae. Irs are found exclusively in the OSNs of coeloconic sensilla and indeed are dependent on the expression of the gene *atonal* that specifies development of the sacculus and coeloconic sensilla[54]. Two Ir genes, *Ir8a* and *Ir25a*, are broadly expressed in coeloconic sensilla and may act as co-receptors for other Ir genes, similar to Orco[55]. Unlike Ors, Irs do not show desensitization to their ligands[56].

SNMP1

Sensory neuron membrane protein (*SNMP1*) is a *Drosophila* homolog of the CD36 scavenger receptor that functions in the uptake of lipoprotein complexes in humans. Expression of *Drosophila SNMP1* is exclusive to the olfactory system and is found only in the neurons of trichoid and intermediate sensilla, with one exception in a neuron of the ab4 sensillum[57]. The Smith lab originally identified *SNMP1* in a screen for mutants affecting the response of Or67d neurons to cVA[58]. The screen yielded several mutants of known components of cVA sensing, including *Or67d* and *Orco*. All identified mutants showed insensitivity to cVA but retained spontaneous activity, indicating that the neuron itself was not compromised by the mutation. One mutant, later identified as *SNMP1*, showed a significant increase in spontaneous activity. Further work showed that these neurons could be activated by higher doses of cVA, but this was coupled with delayed deactivation of the neuron. Similar deactivation defects were observed with the intermediate Or83c neuron that is tuned exclusively to farnesol[20]. To date these are the only *Drosophila* neurons known to be affected by *SNMP1* expression.

Work from the Montell lab has provided more insight into the role of *SNMP1* in cVA sensing[59]. A key feature of these experiments was the rearing of female pupae in isolation from males to remove environmental sources of cVA[59]. These females showed normal spontaneous activity, and when tested for cVA sensitivity they showed both delayed activation and deactivation kinetics[59]. Or67d neurons lacking *SNMP1* show a dramatically prolonged response to cVA, with spiking persisting up to 10 minutes after odorant presentation[59]. Li *et al*. propose that SNMP lowers the energy barrier for pheromone association and dissociation, hence the change in kinetics. The apparent prolonged activation of Or67d neurons by cVA in *SNMP1* mutants indicated a failure of cVA molecules to rapidly dissociate from the receptor complex.

The SNMP1 protein has a large (~420 amino acid) ectodomain containing 6 cysteine residues predicted to form 3 disulfide bridges. In 2016 Gomez-Diaz *et al*. determined that these residues are critical for SNMP1 function in the Or67d neuron, and in some cases for localization of SNMP1 to the cilia of the neuron[60]. These findings were consistent with prior unpublished work from the Smith lab. Gomez-Diaz *et al*. also developed a predicted structure of the SNMP1 ectodomain using the X-ray crystal structure of the ectodomain of mammalian CD36 protein LIMP-2[61]. LIMP-2 shows an internal "tunnel" spanning most of the ectodomain that Gomez-Diaz *et al*. predicted would also occur in the SNMP1 protein. They subsequently introduced point mutations to physically block the putative SNMP1 tunnel using tyrosine. Indeed, the tyrosine mutants showed similar responses to *SNMP1* mutants, though immunohistochemistry determined that this mutated *SNMP1* was still trafficked to the cilia. Gomez-Diaz *et al*. proposed a model of cVA sensing in which cVA molecules are "funneled" through SNMP1 to the lipid bilayer of the neuron, or to the ligand-binding domain of the Or67d receptor. However, there is no indication that the flies used are virgin females reared in isolation to minimize the influence of environmental cVA on their electrophysiological experiments, and the mutants they generated do not really establish the validity of their model. *SNMP1* is an important factor in cVA sensitivity, but its precise mechanism of action remains unclear.

MECHANISMS OF *DROSOPHILA* ODORANT SIGNAL TRANSDUCTION

Odorant receptors are ligand-gated ion channels

The requirement of ORCO for proper localization of other Ors suggests the formation of a heteromeric receptor complex. In 2008 two groups simultaneously but independently identified the Orco-Or complex as a heteromeric ligand-gated ion channel[43, 47]. In both of these studies, *Orco* and an *Or* were expressed in heterologous cells. Sato *et al*. expressed Or83b and Or47a in HeLa cells and used both electrophysiological recordings and calcium imaging to demonstrate an increase in intracellular Ca^{2+} following odorant stimulation. Stimulation with a non-activating ligand does not evoke an increase in Ca^{2+}, indicating that the channel is gated—presumably by the Or that confers the tuning of the preparation. Wicher *et al*. arrived at similar conclusions as Sato *et al*. using HEK293 cells to express *Orco* and *Or22a*. They observed an odorant-dependent increase in intracellular Ca^{2+} as well as a rapid inward current indicating the opening of a ligand-gated ion channel.

Why are insect odorant receptors ligand-gated ion channels rather than GPCRs? One possible explanation is physiology. Terrestrial vertebrates actively sample their odor environments by drawing air across the olfactory epithelium[62]. Insects, however, passively receive olfactory information as they fly through the air. Ligand-gated ion channels show a significantly shorter latency to activation—Sato *et al*. measured the current latency of Or47a-Orco-expressing HeLa cells at 17.9 ± 3.1ms. In comparison, vertebrate olfactory neurons that are GPCRs show a current latency of 50-200ms. The shorter latency of ligand-gated ion channels would allow the fly to rapidly detect changes in odorant identity or concentration as it moves through the air and continuously samples its chemical environment. Such rapid response times could be critical to effective detection of volatile compounds or maintenance of chemotaxis.

The role of G-proteins in odorant signal transduction

Although insect Ors are not "traditional" GPCRs, Wicher *et al*. argue the existence of a second, slower mechanism of odorant signal transduction via G proteins. When stimulating their cells with odorant, they observed a larger, slower inward current dependent on internal ATP and GTP. The requirement of ATP and GTP for the slower current suggests the involvement of G proteins in a metabotropic odorant-induced signal. However, Sato *et al*. did not observe any effects of nucleotides[47]. The heterologous cell preparation was modified to include ion channels to act as reporters of G-protein activation. Co-expression of the cAMP-sensitive CNGA2 human cyclic-nucleotide gated channel revealed a dose-dependent increase in CNGA2 current. Interestingly, intracellular application of a G-protein inhibitor substantially reduced the sensitivity of the preparation to odorant. The metabotropic signaling pathway is therefore more sensitive to odorant, but slower to respond.

There is some evidence for the function of G proteins in the olfactory system, consistent with the OR family's broad similarities to GPCRs. G proteins are expressed in chemosensory antennae, and expression of G subunit blocking factors in OSNs using *Orco*-GAL4 diminished the responses of a subset of olfactory neurons[63-66]. Notably, the metabotropic current observed by Wicher *et al*. occurs roughly 90 seconds after the initial ionotropic current. G proteins may therefore function in a secondary system that is triggered by prolonged odorant exposure.

ODORANT BINDING PROTEINS

Odorant binding proteins (OBPs) were discovered during an experiment intended to find the receptors for moth pheromone[67]. Vogt *et al*. synthesized a radiolabeled version of the *Antheraea polyphemus* pheromone that was able to activate pheromone-sensitive sensilla *in vivo* during electrophysiological recordings. Antennal homogenates were incubated with radiolabeled pheromone, followed by SDS PAGE[67]. Surprisingly, the radiolabeled pheromone bound to a 15kD protein. This protein was present when sensillum lymph alone was isolated from the antennae, indicating that this is a secreted protein and not a membrane-bound receptor[67]. Vogt *et al*. named these pheromone binding proteins (PBPs) and proposed a role in the rapid removal of pheromone from the receptor complex and its degradation in the sensillum lymph. This rapid deactivation would be essential to allow a male to maintain sensitivity to increasing concentrations of female moth pheromone as the male chemotaxes towards the female. Immunolabeling later revealed that these proteins are secreted by the support cells rather than the neuron itself[68]. OBPs are incredibly abundant in the antennae, and have been found at concentrations up to 10mM[69].

Although Vogt *et al*. initially named these PBPs; here I use OBPs to broadly describe the entire family of soluble binding proteins secreted into the sensillum lymph of chemosensory organs. Some OBPs are indeed dedicated pheromone binders with expression restricted to a single sex[67]. Others are expressed in both sexes and bind a range of odorants thought to originate from food sources rather than other members of the species[70, 71].

Initially, other OBPs were identified only in other moth species whose large antennae facilitated the extraction of unidentified proteins. Amino acid sequencing of putative *Antheraea*

pernyi PBPs and comparison with the known *Manduca sexta* PBP sequence revealed the conservation of 6 cysteine residues across all three PBPs[72]. The discovery of conserved cysteine residues facilitated more rapid identification of OBPs across numerous insect species by isolating antennae-specific proteins and comparing their amino acid sequences[71, 73]. A second class of chemosensory proteins, or CSPs, has only 4 conserved cysteine residues and is not considered part of the OBP family[74].

The first 3 dimensional model of an OBP was resolved via X-ray diffraction analysis of the *Bombyx mori* PBP complexed with its ligand, the moth pheromone bombykol[75]. The structure consists of 6 alpha-helices in a roughly conical formation. Four of the antiparallel helices converge to form a hydrophobic binding pocket, with another helix forming the "cap" of the pocket.

How do OBPs function? There are several theories: 1) deactivation of odorant response, 2) transport of odorant molecules through the sensillum lymph, and 3) protection of odorant molecules from premature degradation. Vogt *et al*. initially proposed a role for OBPs in rapid deactivation of OSNs by removal of the ligand from the receptor complex. Later assays with known esterases that degrade pheromone revealed that esterase alone rapidly degraded pheromone molecules independent of the presence of known PBPs[76]. OBPs therefore might function in the transport of pheromone and odorant molecules rather than in their degradation. The *B. mori* PBP-bombykol structure provides some evidence for this theory: at lower pH the PBP-bombykol complex adopts a "relaxed" conformation allowing bombykol to easily move from the binding pocket. This pH-dependent change may reflect sensitivity to the lower pH at the surface of the neuronal membrane that would facilitate release of the pheromone onto the

receptor complex[75, 77, 78]. Alternately, OBPs might protect odorant molecules from degrading enzymes prior to the activation of the neuron[79]. A role in deactivation is still possible for some OBPs, but has never been definitively demonstrated[14, 80].

Drosophila OBPs: the case of LUSH

The OBP *lush*, also called *Obp76c* and later renamed *Obp76a*, was originally identified by the Smith lab in an enhancer trap screen for antennae-specific genes[81]. The enhancer trap line *ET249* showed expression of LacZ restricted to the dorso-lateral region of the funiculus. Interestingly, the axons of olfactory neurons were not labeled in this line, but closer examination of fine sensillar structure showed that *ET249* was expressed in the trichoid support cells of the sensillum. The gene of interest was mapped to position 76c on the third chromosome.

A mutant for this gene was generated by using P-element excision to remove 3kb of genomic DNA encompassing the *lush* region. An olfactory trap assay was used to compare the responses of control and mutant lines to a range of 60 volatile compounds. Mutant flies showed an increased attraction to high concentrations of alcohols, hence the name *lush*. This behavior could be reversed by introducing a transgenic copy of lush into the mutant line[81]. Analysis of the *lush* sequence revealed a signal sequence and 6 conserved cysteine residues, the hallmarks of OBPs. Staining of antennal sections with a LUSH-specific antibody labeled the shafts of trichoid sensilla, indicating that LUSH is a secreted protein[81].

Lush expression is restricted to the trichoid class of sensilla, of which there are two members[81, 82]. As previously noted, at1 sensilla house a single OSN expressing Or67d that is

tuned exclusively to the male pheromone cVA. *Lush* mutants show a significant decrease in sensitivity to cVA, suggesting that *lush* is required to transport the hydrophobic pheromone molecules through the aqueous sensillum lymph[11]. Weak activation is achieved with 100% cVA, but this activation is substantially delayed compared to the control. Importantly, sensitivity can be restored when recombinant LUSH protein is infused into the sensillum via the recording pipette. *Lush* is therefore not required for the development of the OSN, but is sufficient to restore cVA sensitivity. *Lush* mutants also show diminished spontaneous activity in the absence of cVA, reduced from approximately 1 spike/second to 1 spike/200 seconds. Spontaneous activity could also be restored through infusion of recombinant LUSH into *lush* mutant sensilla, suggesting that LUSH is also necessary and sufficient for the spontaneous activity of Or67d neurons. A key feature of this experiment is the amount of LUSH protein infused into the sensillum—the total concentration used in rescue experiments was approximately 180nM. In contrast, the concentration of an OBP in a given sensillum is estimated at 10mM, a nearly 10-fold increase. The requirement of a low dose of recombinant LUSH suggests that, while OBPs are abundantly expressed in the sensillum, the required total concentration of OBPs in the sensillum lymph is far lower.

Crystallographic structures of LUSH show that, like *B. mori* PBP, the protein forms 6 alpha helices surrounding a hydrophobic binding pocket[83]. Unlike *B. mori* PBP, LUSH maintains its conformation at a lower pH. The X-ray crystal structure of LUSH bound to cVA reveals several unique features of the bound conformation[84]. F121 interacts with cVA to produce a conformational shift at the enclosed end of the binding pocket. The mutant F121A is predicted to prevent or reduce a cVA conformational shift without altering the binding of cVA to LUSH.

Infusion of F121A LUSH into the at1 sensillum of a *lush* mutant is 5-fold less active in restoring cVA sensitivity, while spontaneous activity is restored to wildtype level[84]. Therefore, while F121 is important for the cVA-induced conformational change, it is not critical for the changes in spontaneous activity observed in the null mutant. Another notable feature of unbound LUSH is a salt bridge formed between D118 and K87. When cVA is bound, this salt bridge is disrupted. A D118A mutant was used to disrupt the formation of the salt bridge and generate a "constitutively active" LUSH conformation. Infusion of this "active" LUSH restored cVA sensitivity to levels comparable to wildtype, while spontaneous activity in the absence of cVA was significantly increased above wildtype levels. Resolution of the crystal structure of D118A LUSH shows that its conformation is similar to that of cVA-bound LUSH. The conclusion from these studies is that the cVA-bound LUSH appears to act as a ligand for the Or67d receptor complex. In the absence of cVA, it is possible that LUSH can spontaneously undergo a shift to its active conformation, eliciting weak firing that is observed as spontaneous activity of the neuron. However, transgenic flies expressing LUSH D118A in lieu of wild type LUSH had only a 2-fold increase in spontaneous activity. Therefore, either disruption of the salt bridge has minimal effect on the ability of LUSH to directly activate Or67d neurons, or the flies apply homeostatic mechanisms to normalize the spiking in the presence of dominant LUSH[85].

A key feature of the previously described experiments was the use of a single male to define "environmental" cVA exposure. It is essential to understand what physiological cVA concentrations are, and to insure we are using biologically relevant stimuli. Briefly, a single decapitated male was fixed on a micromanipulator with its abdomen oriented to the SSR preparation. When a single male abdomen was 1cm from a naïve virgin female fly, a response

was elicited from Or67d neurons. The approach of a single male abdomen was used to correlate the spike frequencies of this *bona fide* stimulus to different cVA dilutions impregnated on filter paper with air passed over the paper to elicit similar spiking frequencies from the Or67d neurons that now comprise the Smith lab's standard cVA dose-response curve. The response of an Or67d neuron to 300ms of air passed over 30µL of 0.03%-30% cVA om filter paper is the standard for "physiological" cVA exposure.

Gomez-Diaz *et al*. argue that LUSH is not strictly required for the transport of cVA to the Or67d receptor complex[86]. They generated a set of transgenic flies expressing the mutated versions of *lush* used by Laughlin *et al*. They identified no significant changes to the sensitivity or spontaneous activity of Or67d neurons using these *lush* variants, when compared to a standard *lush* rescue. However, their electrophysiological assay differs significantly from that used in previous experiments. The end of the odor delivery tube was positioned 15mm away from the preparation, where Laughlin *et al*. positioned the tube 1cm away. They also demonstrated that the requirement for lush could be bypassed using a "close-range" approach in which the odorant tube is positioned 0.1mm from the antennal segment. While this experiment indeed confirms activation of Or67d neurons by cVA in the absence of LUSH, and that LUSH is required to detect physiological levels of cVA, it does not necessarily reflect the experience of a fly under physiological conditions, where such close proximity is unlikely to occur. The precise mechanism by which LUSH sensitizes Or67d neurons to cVA remains unknown.

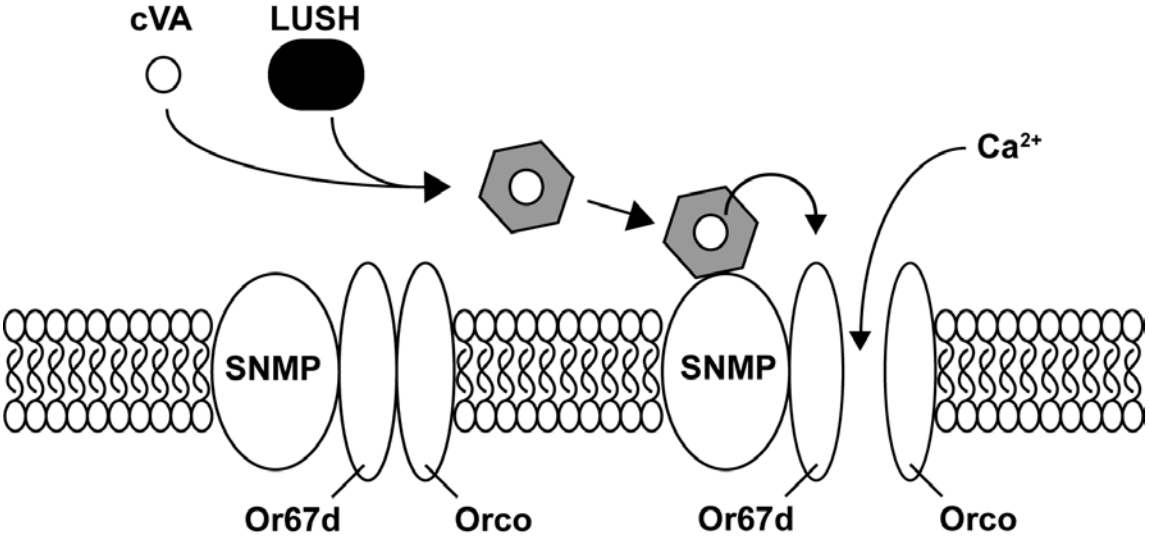

Figure 2-2. A model for cVA sensing and the role of LUSH. LUSH exists in a distinct conformation in the absence of cVA. Or67d and Orco heterodimerize on the dendrite to form a ligand-gated ion channel. When cVA is present, LUSH binds a cVA molecule and undergoes a conformational change. The LUSH-cVA complex interacts with the Or67d receptor complex, releasing the cVA molecule. Binding of cVA to the receptor complex triggers activation of the neuron. In the absence of cVA, the LUSH protein can spontaneously adopt its active conformation and interact with the receptor complex, causing weak neuronal activation observed as spontaneous activity.

Other OBPs in *Drosophila*

In 2001 the Smith lab searched the *Drosophila* genome to identify additional OBP genes. They also conducted a large-scale screen of the expression of all the OBP genes they identified using a LacZ fusion construct[87]. X-gal staining facilitated the identification of the expression patterns of these different OBPs. Indeed, some OBPs are expressed exclusively in the antennae, while others are not expressed in the antennae at all. Organs expressing OBPs include the mouth parts, legs, genitalia, and wing margins, all of which have some putative chemosensory function. The OBPs expressed on the antennae showed identified unusual patterns across the funiculus that could theoretically be associated with specific sensillum subtypes. The completed genome sequence eventually revealed there are a total of 51 members, nearly equal to the 62 known *Drosophila* odorant receptors[88].

Recently Larter *et al*. set out to identify the expression patterns of the ten most abundantly expressed OBPs in *Drosophila*[89]. RNA *in situ* hybridization was used to label OBPs of interest in flies expressing GFP driven by an *Or* gene specific to one of the ten basiconic sensilla or to the trichoid sensilla. The same method was also used with flies expressing GFP in either thecogen or tormogen cells to identify which support cells produce which OBPs. There are several limitations to their methodology. RNA *in situ* hybridization confirms the presence of RNA of the genes of interest, but does not indicate expression of the mature protein. Secondly, their representative *Or* genes do not include intermediate or coeloconic sensilla.

The functional roles of OBPs have largely been characterized using odorant behavior screens[90]. In these screens, UAS-RNAi lines specific to different OBPs are driven by a ubiquitous *tubulin*-GAL4 and the resulting flies are against a panel of odorants to measure changes in attraction or aversion. The use of RNAi presents a significant barrier to the efficacy of these screens, as some lines showed no significant suppression of the transcript[91]. Furthermore, the odorants used in the screen tend to be broadly detected by multiple classes of OSNs, further obfuscating potential specific interactions between OBPs and Ors. While these broad screens have not provided insight into the specific mechanisms of individual OBPS, a select number of *Drosophila* OBPs have been sufficiently characterized to define their role and interaction with a given chemosensory neuron.

Obp49a

OBPs are found in many organs with putative chemosensory functions, particularly in the mouthparts. Jeong *et al*. identified four OBPs enriched in the gustatory sensilla, and generated mutants to each individual OBP[92]. These mutants were tested in a choice assay between two sucrose solutions of different concentrations. They were then tested using a high concentration of sucrose mixed with bitter compounds, or a lower concentration of sucrose without the bitter compound. Although higher sucrose concentrations are more attractive to flies, the presence of a bitter compound causes the flies to lose attraction to the higher sucrose concentration. Flies lacking *Obp49a* did not have the typical repulsion to the high sucrose + bitter mixture, and indeed lacked avoidance to a number of bitter compounds. Electrophysiology on gustatory sensilla housing sweet-sensing GRNs showed no difference when sucrose was applied to control

or mutant flies, suggesting that *Obp49a* is not required for sweet sensing. However, the same test on bitter-sensing neurons showed normal responses as well, suggesting a more complex role for this OBP in gustation.

Electrophysiological recordings were performed on L-type sensilla that house 4 GRNs sensitive to sugar, water, low salt, or high salt. The lack of bitter-sensing neurons facilitated the study of inhibition of sweet-sensing GRNs by bitter compounds. They demonstrated that combining bitter compounds with the sucrose delivered to the GRN inhibited the sucrose response in a dose-dependent manner, indicating that bitter compounds suppress sucrose sensation. However, this inhibition is abolished in the *Obp49a* mutants.

How does an OBP inhibit the response of a GRN to sucrose when a bitter tastant is present? Jeong *et al*. purified OBP49a from head extracts and used surface plasmon resonance to measure the binding of OBP49a to both sweet and bitter compounds. While OBP49a showed dose-dependent binding to bitter compounds including berberine and quinine, no binding to sucrose was observed. This suggested that OBP49a directly interacts with bitter compounds to suppress the activity of sweet-sensing GRNs. To demonstrate this Jeong *et al*. generated a membrane-tethered *Obp49a* that would be expressed on the surface of the cell of choice. This construct was sufficient to restore aversion to sucrose in the presence of bitter compounds, but only when the tethered OBP was expressed in sweet-sensing GRNs. At least one *Drosophila* OBP is therefore required for the suppression of sweet sensing in the presence of a bitter tastant. They propose two possible models for the inhibition of sweet-sensing GRNs in the presence of bitter tastants. In one, OBP49a binds to bitter tastants and physically blocks the ligand-gated ion

channel tuned to sucrose. Alternately, OBP49a transports the bitter tastant to the membrane to increase its concentration at the receptor complex, thereby outcompeting sucrose for binding.

Obp28a

The OBP expression screen conducted by Larter *et al*. identified a basiconic sensillum class expressing only one OBP abundantly[89]. Per their expression screen, ab8 sensilla only express the OBP *Obp28a*, though the OBP itself is expressed across multiple sensilla. CRISPR was used to generate an *Obp28a* null mutant. Mutants were then electrophysiologically screened for changes in response to the hydrophobic odorant 1-octanol. Both neurons in the sensillum were included in the calculation of response, due to apparent difficulties in distinguishing neuron identity based on amplitude and frequency. Unlike *lush* mutants, no changes in spontaneous activity were observed. Surprisingly, the mutants did not show reduced sensitivity to 1-octanol but instead showed a more robust response across a range of concentrations. Traces were binned into 50ms intervals to plot the response as a peri-stimulus time histogram (PSTH) to examine both activation and deactivation kinetics. The PSTH plot showed that while mutant activation kinetics remained normal, the peak activation was significantly higher. To address the possibility that OBP28a functions in sensillum lymph clearing, they next presented 1-octanol for 30 seconds and observed the deactivation kinetics. Surprisingly, *Obp28a* mutant neurons deactivated more rapidly that control flies[89].

Larter *et al*. next devised a “pulse” assay in which a sustained background of 1-octanol was maintained while a second 1-octanol sample was pulsed onto this preparation for a brief

period of time. Under this paradigm, *Obp28a* mutants still show robust responses to the pulse of odor, even in a high odor background[89]. These findings suggest that OBP28a acts as a buffer for ab8 neurons: when a large number of odorant molecules enter the sensillum lymph, OBP28a binds some of these molecules to prevent their reaching the receptor complex (Figure 2-3). If OBP28a were competing with the receptor complex for ligand, we would assume a decrease in activation latency that is not observed even at low concentrations of odorant. The mechanism by which OBP28a acts as a buffer therefore remains uncertain. Larter *et al*. furthermore do not show any experiments to rescue the mutant phenotype by transgenic expression of the *Obp28a* gene, which would establish the necessity and sufficiency of OBP28a as an odorant buffer[89].

OBP59a

Obp59a is expressed in a region of the antenna associated with the sacculus. The sacculus is a cavity in the funiculus that mediates humidity sensing, or hygrosensation, that is detected by a subset of coeloconic sensilla[28, 93, 94]. Humidity detection can be assayed by testing a fly's preference for low or high salt concentrations, where high salt concentration yields a drier environment that is generally less attractive to flies. Deletion of *Obp59a* by CRISPR increases tolerances of less humid environments; indeed, mutant flies even show a preference for lower humidity[95]. Transgenic expression of *Obp59a* restored the sensitivity of mutant flies to their environmental humidity, thereby establishing the necessity and sufficiency of *Obp59a*. The precise mechanism of hygrosensation by coeloconic sensilla is not yet known, nor is it understood why an OBP would be essential to the detection of environmental humidity. A model consistent with previous models from the Smith lab is that OBP59a undergoes a conformational

change in response to reduced osmolality. Nonetheless, a role for an OBP in the detection of a readily soluble environmental cue was previously unprecedented. The location of hygrosensitive sensilla in the sacculus precludes electrophysiology, but the highly specific expression of *Obp59a* suggests a specific role in hygrosensation.

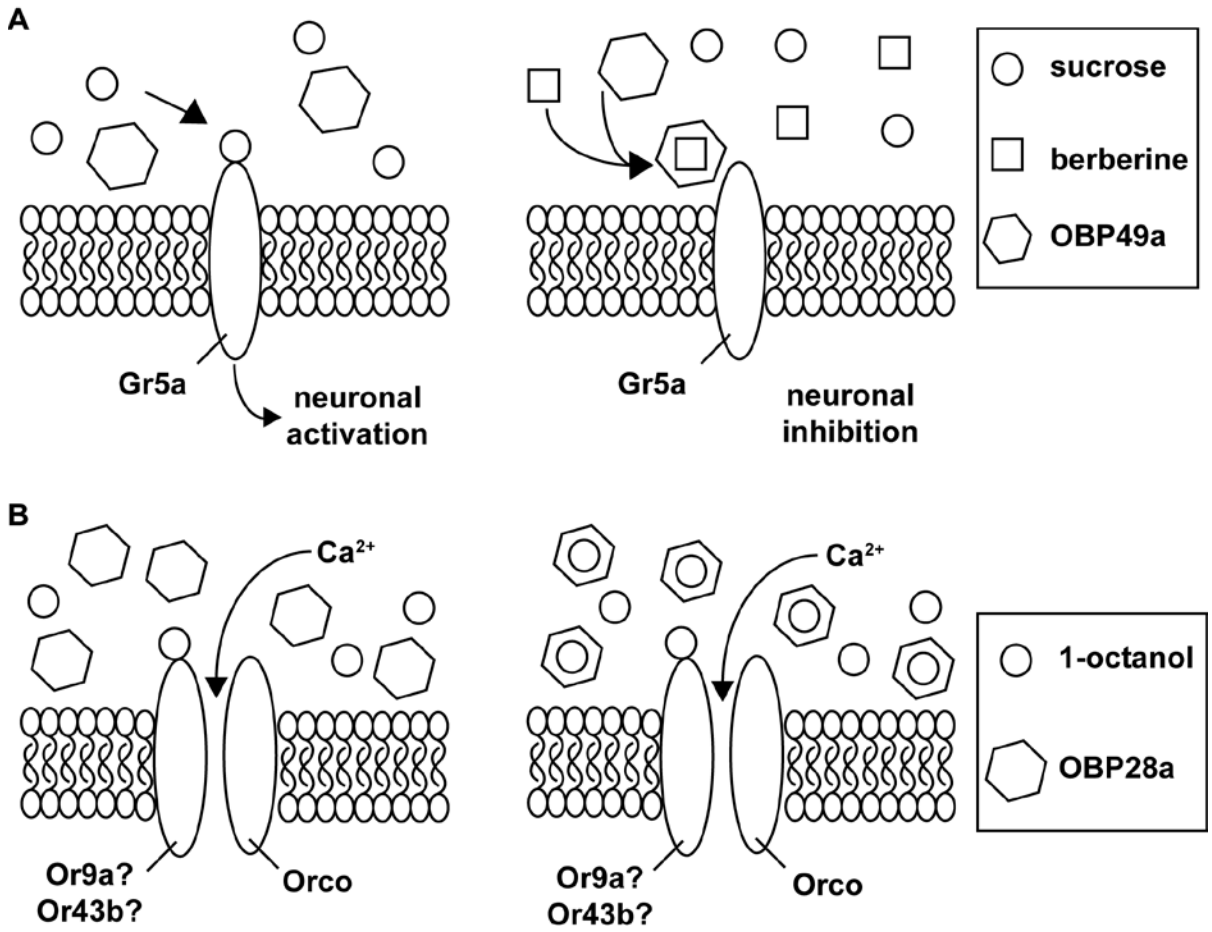

Figure 2-3. Proposed models for the function of *Drosophila* OBPs *Obp49a* and *Obp28a*. A. Right, cartoon showing the activation of *Gr5a*-expressing neurons in response to sucrose. OBP49a does not bind sucrose molecules. Left, cartoon showing the sucrose response is inhibited when a bitter tastant is also present. OBP49a binds bitter tastants and may inhibit the response to sucrose by either blocking the sucrose receptor or transporting bitter tastants to the surface of the membrane to increase competition for binding. B. Right, cartoon showing the activation of ab8 neurons in response to 1-octanol. Left, when high concentrations of 1-octanol are present, OBP28a binds excess molecules to buffer the response.

OS-E and OS-F

OS-E (*Obp83b*) and *OS-F* (*Obp83a*) were the first OBPs identified in *Drosophila*[96]. McKenna *et al*. used subtractive hybridization to isolate a set of antennae-specific cDNAs and characterize their expression on the antennae[96]. *OS-E* and *OS-F* showed high similarity to known OBPs of other insect species and were expressed on the dorso-lateral region of the funiculus associated with trichoid sensilla. These OBPs show an unusual degree of amino acid sequence similarity, nearly 70%. They are also located less than 1 kilobase apart, consistent with a recent gene duplication event[74, 96]. Because of this similarity, antibodies generated to OS-E were cross-reacted to OS-F, and vice versa, to eliminate nonspecific staining. Staining with individual antibodies on serial sections of the antennae reveal that OS-E and OS-F are always co-expressed[97]. Both OBPs are co-expressed in trichoid sensilla, determined by co-labeling with LUSH, but are also found in a subset of sensilla dispersed among trichoids[82]. Initially these sensilla were identified as basiconics, but have since been recognized as intermediate sensilla.

Although these were the first *Drosophila* OBPs identified, their function is unknown. It is not known if their co-expression indicates a redundancy of function, or if they have unique roles in spite of their high degree of sequence similarity.

.

Table 2-1. Olfactory sensilla of the antennae, identity of OSNs, and best known ligands[15-17, 26, 30]

Class	Subtype	Receptors in each neuron	Strongest reported activator
large basiconic	ab1	Or42a	ethyl propionate
		Or92a	2,3-butanedione
		Gr21a/Gr63a	CO_2
		Or10a	methyl salicylate
	ab2	Or59b	methyl acetate
		Or85a/Or33b	ethyl 3-hydroxybutyrate
	ab3	Or22a/Or22b	ethyl hexanoate
		Or85b	6-methyl-5-hepten-2-one
small basiconic	ab4	Or7a	E2-hexenal
		Or33a/Or56a	geosmin (Or56a)
	ab5	Or82a	geranyl acetate
		Or33b/Or47a	pentyl acetate
	ab6	Or85b/Or98b	6-methyl-5-hepten-2-one (Or85b)
		Or49b	2-methylphenol
	ab7	Or98a	ethyl benzoate
		Or67c	ethyl lactate
	ab8	Or9a	3-hydroxy-2-butanone
		Or43b	ethyl-trans-2-butenoate
	ab9	Or67b	acetophenone
		Or69aA/Or69aB	?
	ab10	Or49a/Or85f	2-heptanone
		Or67a	phenylethyl alcohol
trichoid	at1	Or67d ($SNMP^+$)	11-cis vaccenyl acetate
	at4	Or47b ($SNMP^+$)	trans-2-hexenal
		Or88a ($SNMP^+$)	2-octanone
		Or65a/Or65b/Or65ac ($SNMP^+$)	hexanol
intermediate	ai1	Or13a ($SNMP^+$)	1-octen-3-ol
	ai2	Or83c ($SNMP^+$)	farnesol
		Or23a ($SNMP^+$)	1-pentanol
	ai3	Or19a/Or19b ($SNMP^+$)	limonene
		Or2a ($SNMP^+$)	isopentyl acetate
		Or43a ($SNMP^+$)	1-hexanol
coeloconic	ac1	Ir31a	ammonia
		Ir75d	
		Ir92a/Ir76b	
	ac2	Ir75a	1,4-diaminobutane
		Ir75d	
		Ir76b	
	ac3	Ir75a/Ir75b/Ir75c	propanal

		Or35a/Ir76b	hexanol
	ac4	Ir84a	phenylacetaldehyde
		Ir75d	
		Ir76a/Ir76b	

Table 2-2. *Drosophila* OBPs and their expression in adult chemosensory organs[74, 81, 82, 87, 89, 92, 96, 98, 99]

OBP	Antennae	Maxillary palps	Labellum	Wings	Tarsi
8a	ND	ND	ND	ND	ND
18a	NS	NS	NS	NS	NS
19a	+	-	-	-	-
19b	-	-	-	+	+
19c	-	-	-	-	-
19d	+	+	+	ND	ND
22a	-	-	-	-	-
28a	+	-	-	NS	NS
44a	ND	ND	ND	ND	ND
46a	ND	ND	ND	ND	ND
47a	-	-	-	-	-
47b	ND	ND		ND	ND
49a	ND	ND	+	ND	ND
50a	ND	ND		ND	ND
50b	ND	ND		ND	ND
50c	ND	ND		ND	ND
50d	ND	ND		ND	ND
50e	ND	ND		ND	ND
51a	-	-	-	-	-
56a	NS	NS	NS	NS	NS
56b	-	-	-	-	-
56c	+	-	-	+	-
56d	+	+	-	+	+
56e	+	-	+	-	-
56f	-	-	-	-	-
56g	-	-	-	-	-
56h	+	-	+	-	-
56i	-	-	-	-	-
57a	+	+	-	-	-
57b	+	+	-	+	+
57c	+	+	+	-	-
57d	-	-	-	-	+
57e	-	-	-	-	+
58a	ND	ND	ND	ND	ND
58b	ND	ND	ND	ND	ND
58c	ND	ND	ND	ND	ND
58d	ND	ND	ND	ND	ND

59a	+	ND	ND	ND	ND
69a	+	-	-	ND	ND
76a (LUSH)	+	-	-	-	-
83a (OS-F)	+	-	-	ND	ND
83b (OS-E)	+	-	-	ND	ND
83c	-	-	+	-	-
83d	-	-	-	-	-
83e	ND	ND	ND	ND	ND
83f	NS	NS	NS	NS	NS
83g	-	-	-	-	-
84a	+	-	-	ND	ND
85a	ND	ND	ND	ND	ND
99a	NS	NS	NS	NS	NS
99b	+	+	-	-	-

ND, not determined. NS, not specific. Not specific indicates staining of the cuticle that is not associated with the chemosensory organs.

CHAPTER THREE
Methodology

DROSOPHILA STOCKS

Wild type is an isogenized w^{1118} strain (Bloomington Stock Center, BS3605). *OS-E/F* mutants were backcrossed for 5 generations to this stick to minimize genetic background effects. *Nos>Cas9* flies were generated by Kondo *et al*[100]. *Hsp70>Cre* flies were obtained from the Bloomington Stock Center (BS34516) and were used to delete the *Lox-3xP3>RFP-Lox* marker from the deletion mutants. *Or47b* mutants were described in by Wang *et al*[101]. *Or88a* and *Or65abc* mutants are described in Pitts *et al*., and the *Or83c* mutants ($Or83c^{MB11142}$) are described in Ronderos and Smith[20, 25]. The *lush* mutants ($lush^{1}$) were described by Kim[81]. Flies of both sexes were used in these experiments.

Generation of CRISPR/Cas9 Mutants

CRISPR targets were identified upstream and downstream of the *OS-E* and *OS-F* genes using the CRISPR Optimal Target Finder[102] (Figure 3-1 A). Overlapping oligonucleotides were annealed for each target site and cloned into pU6-Bbs1-chiRNA plasmid[102]. Approximately 1 kb of sequence upstream and downstream of the cleavage targets were cloned using PCR and inserted into pHD-DsRed-attP (Addgene). The DNAs were diluted to a final concentration of 20ng/µl for the U6 DNAs and 250µg/µl for the targeting DNA in injection buffer (1mM NaPO4, 50mM KCl, pH 6.8). All DNAs were injected into *Nos>Cas9* embryos and the resulting flies

were crossed to Balancer Chromosome stocks (*TM6b*)[100]. The balanced progeny were screened for RFP expression in the eye.

Independent mutant lines were established from three lines, and all were homozygous viable and fertile. The phenotypes reported here were confirmed in independent lines. Correct insertion of the *3xP3>RFP* donor construct was confirmed via PCR where one primer was internal to the RFP donor construct and one was external to the region of homology (Figure 3-1 A-B). Primers specific to the coding regions of either *OS-E* or *OS-F* were also used to confirm absence of the targeted genes (Figure 3-1 A-B). Cre recombinase was used to excise *3xP3>RFP* from *OS-E/F* mutant stocks, and the resulting flies used in some experiments. No differences in phenotype were observed whether *3xP3>RFP* was present or not.

Primers used for mutant generation and validation

CRISPR upstream target oligonucleotides

5’CTTCGGCCCTTTTATGAGATTACT

5’AAACAGTAATCTCATAAAAGGGCC

CRISPR downstream target oligonucleotides

5’CTTCGTCAAGAGTTGTTTGCGCCG

5’AAACCGGCGCAAACAACTCTTGAC

Upstream homology domain primers

5’GCATGCCTGGTGCAGTTGCTGTTGCATCGG

5’GCGGCCGCATTACTGGGGCTCCATTTC

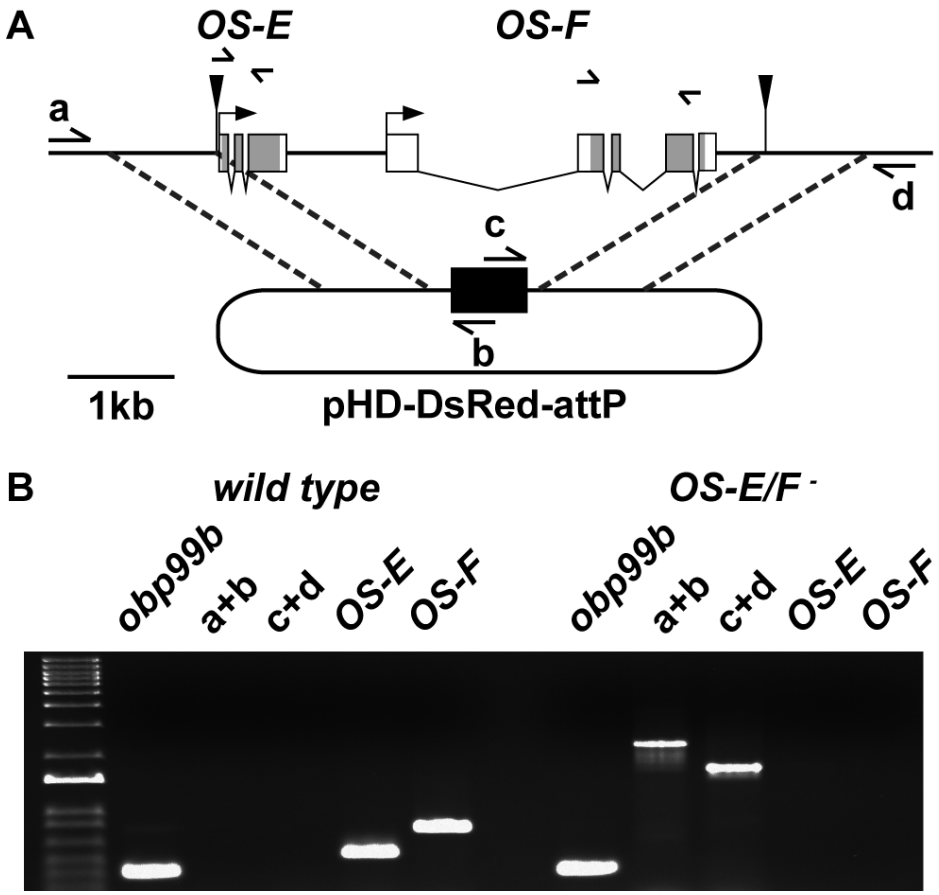

Figure 3-1. Generation of an *OS-E/F* deletion mutant. A. Map of the *OS-E/F* genomic region on the right arm of the third chromosome. CRISPR-mediated replacement of the *OS-E* and *OS-F* genes with *3xP3>dsRed* is depicted. Solid triangles indicate the position of CRISPR-Cas9 cleavage sites. The dashed lines denote the regions of homology upstream and downstream of the OBP genes that were cloned into the donor vector (see Materials and Methods for details). Labeled arrows indicate the position and orientation of primers for PCR reactions used to identify correct integration of the DsRed gene (black rectangle) into the *OS-E/F* locus. Unlabeled arrows indicate gene specific primers used to determine presence of the *OS-E* and *OS-F* genes. B. Agarose gel image of PCR fragments generated with the primers depicted in panel 1A. PCR fragment sizes from control and *OS-E/F* mutant confirm correct integration of the DsRed gene and loss of the *OS-E* and *OS-F* genes in the mutant. Markers in left lane are 1 kb ladder (ThermoFisher).

Downstream homology domain primers

5’ACTAGTGCGCCGTGGCAAAAACTTGTATAAAAAC

5’CTCGAGTAAATTTAAAAATCTTTGACTTTAATTCG

Primers to validate upstream integration

5’AATTATATTGCCCCATCCCC

5’CGATGAACTTCACCTTGTAG

Primers to validate downstream integration

5’CGCGACTCTAGATCATAATC

5’CCTTCCAGGGAATAAAGTAC

Primers to specific to the *OS-E* gene

5’GGACAGATTTGGTAAGTAGC

5’GAGCCCCAGTAATCTCATAA

Primers specific to the *OS-F* gene

5’TGGCTTTGAATGGCTTTGG

5’ATTGTCGTCCACCACTTCG.

QPCR

RNA was extracted from the antennae of 5-10 day old *Drosophila*. The PicoPure RNA Isolation Kit (Applied Biosystems) was used for RNA extraction. 50 antennae from each genotype were dissected and collected in 50µl of extraction buffer. The antennae were homogenized using Bead Ruptor4 (Omni International) and precipitated in ethanol. DNA

contamination was removed with RNase-free DNase (Qiagen). First-strand cDNA synthesis was performed using First-Strand Synthesis SuperMix for qRT-PCR (Invitrogen). qRT-PCR was performed in an Applied Biosystem 7500 Real-Time PCR System with Fast SYBR Green Master Mix (Applied Biosystems). Three replicates were performed together with a no-RT control (without reverse transcriptase) and a no template control. Melting curve analysis and primer efficiency tests were performed for all primers sets.

Primers for QPCR

Primers specific to *OS-E*

5'GCTCCCAAAACTGGCGTTAC

5'GAGAAGGTCTTGAACGCCATT

Primers specific to *OS-F*

5'CTTTGGTCGGCGTGTCAG

5'CCAAGCCCTTCCACGACG

Primers specific to *EF1* (Ponton)

5'GCGTGGGTTTGTGATCAGTT

5'GATCTTCTCCTTGCCCATCC

Generation of transgenic rescues

A 10.6kb DNA fragment (containing the *OS-E* and *OS-F* genes, and all non-coding DNA extending to the next identified loci) was isolated by high fidelity PCR from wild type DNA. No

other known transcription units were encoded by this fragment, and the correct coding sequences for these two genes was confirmed to lack PCR errors by DNA sequencing. This fragment was cloned into pCasper4 and used to generate transgenic flies as previously described[103, 104]. For single gene rescue, deletions were produced in the rescuing transgene using the Q5 site-directed mutagenesis kit (NEB).

Primers for transgenic rescues

Genomic rescue primers

5’CTCGAGAAGCTGGCAACTGAATCCGA

5’GCGGCCGCTTCGAGTTCCAGTTGCAGTT

Q5 *OS-E* coding region deletion primers

5’TTTGAAACTACAATGAATGG

5’AATTTATTTACATTTATATTAACATTTAATTG

Q5 *OS-F* coding region deletion primers

5’TTTAATGTGGCTCTTTCCGTTTC

5’ACACCTGGGCCACCTTTC

Myc-tagged *OS-E*

The Q5 system was also used to add a *BglII* site into the *OS-E* rescue construct one codon after the predicted signal cleavage site. A 2X Myc tag with a flexible linker (EQKLISEEDLEQKLISEEDL$(GGS)_8$) was inserted in frame by annealing and ligating 4

overlapping oligonucleotides into the *BglII* site and sequencing several clones to identify inserts in the proper orientation.

Primers to generate Myc-tagged OS-E

Q5 primers to introduce BglII site

5'AGATCTCTGGGCAGCGGCACAGCC

5'GAACCAAGGCGCGATGGAGAGG

2x Myc tag

5'GATCTCAGGAACAAAAACTCATCTCAGAAGAGGATCTGGAACAAAAACTCATCTC

A

5'AGATCCTCTTCTGAGATGAGTTTTTGTTCCAGATCCTCTTCTGAGATGAGTTTTTGT

TCCTGA

$(GlyGlySer)_8$ linker

5'GAAGAGGATCTGGGCGGCAGCGGCGGCAGCGGCGGCAGCGGCGGCAGCGGCGGC

AGCGGC GGCAGCGGCGGCAGCGGCGGCAGCA

5'GATCTGCTGCCGCCGTGCCGCCGCTGCCGCCGTGCCGCCGCTGCCGCCGCTGCCGC

CGCTGCCGCCGCTGCCGCCC

SINGLE SENSILLUM ELECTROPHYSIOLOGY

Single sensillum recordings (SSR) were performed on 3-6 day old flies as described in Xu *et al*. except for recordings from at4 sensilla that were performed on 1-3 day old flies[11, 25].

Newly eclosed flies were aged in mixed-sex groups on fresh food vials. A single fly was fixed under a humidified charcoal-filtered air stream (36ml/min, 22-25^{0}C). A reference electrode was placed in the eye, and a recording electrode was placed into an individual sensillum. Signals were amplified 100X (USB-IDAC System; Syntech, Hilversum, The Netherlands) and fed into a computer via a 16-bit analog-digital converter and analyzed offline with AUTOSPIKE software (USB-IDAC System; Syntech).

Odorant sample preparation and presentation

Odorant samples were diluted in paraffin oil, and 30µl was spotted onto a 1cm^2 Wattman paper inserted into a pipet over which the stimulus air pulse was passed into a constant air stream 1.0cm from the fly using a computer-controlled trigger. The percentage identified in figures indicates the dilution of odorant applied to the paper, not the actual stimulus concentration at the preparation. Odorant stimulus lasted for 300ms, except in at4 sensilla where the time of application was extended to 1s[25]. In all cases, a given odorant was only tested once on a single fly, though multiple odorants were tested on single flies.

Spike waveform analysis

Spike waveforms from recordings were sorted based on amplitude and shape using custom software written in MATLAB. Briefly, principle component analysis was used to sort putative spikes identified based on user-defined amplitude thresholds described in Pitts *et al*[25].

2016. Spikes were initially sorted using k-means clustering and were then manually merged into large-amplitude and small-amplitude populations. This analysis gives the precise time of each spike down to milliseconds.

Spontaneous and evoked activity of olfactory neurons

Spontaneous activity (spikes/s) was calculated as the number of spikes per second occurring in a 10 second period prior to odorant presentation, divided by 10. Elicited activity (Δspikes/s) was calculated as the number of spikes occurring in the 1 second following odorant exposure, from which spontaneous activity for the 10 seconds prior to odorant application was subtracted.

Calculating activation and deactivation of olfactory neurons

The deactivation time constant, tau (τ), was calculated by binning individual traces into 50ms intervals. The bin with the largest number of spikes was counted as time point 0 and subsequent bins used to plot the exponential decay curve from which tau was derived. Tau was calculated using the formula $N(t) = Noe\text{-}t/\tau$ where N(t) is the quantity of spikes at time t and τ is the time at which the population of spikes is reduced to 1/e times the initial value. Latency to activation was determined by identifying the time point after odorant presentation at which a cluster of spikes is observed, measured in milliseconds after the initiation of odor presentation. This latency represents the time from activation of the valve initiating the flow of odorant to the

preparation, to arrival of the odorant molecules to the receptors, producing spikes. In the case of Or47b neurons, where spontaneous activity is sufficiently high to obfuscate the occurrence of a spike cluster indicating odorant response, 50ms bins were used starting at the moment of odorant presentation to infer no change in the latency to activation.

IMMUNOCYTOCHEMISTRY

Immunocytochemistry was performed on 10µm sections of frozen *Drosophila* head tissue from both sexes as previously described[58]. A Myc monoclonal antibody (Developmental Studies Hybridoma Bank, Iowa City, IA) was diluted to 1:1000 for immunofluorescence and was detected with Alexa 555 (Molecular Probes). Confocal images were obtained using a Zeiss LSM 510 confocal microscope. A C-terminal Myc-tagged *Acinus* line was used as a positive control[105].

STATISTICAL ANALYSIS

Wild type and mutant genotypes were compared using two-tailed Student t-tests. Multiple genotype values were compared using one-way ANOVA with post hoc Tukey's test to correct for multiple comparisons. Analysis was performed using GraphPad Prism 7 and Origin 8.5 (OriginLab).

CHAPTER FOUR
Results

To understand the roles of *OS-E* and *OS-F* in *Drosophila* olfaction, I generated a null mutant using CRISPR/Cas9 to delete both genes. Deletion of *OS-E* and *OS-F* was confirmed through PCR, and QPCR was also used by Kishor Kunwar to verify complete loss of the transcript (Appendix A).

Antibody staining has demonstrated that *OS-E* and *OS-F* are always co-expressed and localized to a region of the antennae associated with trichoid and intermediate sensilla[82]. Larter *et al*. claim that *OS-E* and *OS-F* are also expressed in a subset of basiconic sensilla, as evidenced by RNA *in situ* hybridization[89]. I generated a transgenic fly expressing Myc-tagged *OS-E* in the null mutant background and used a Myc antibody to examine expression of the mature protein (Appendix B). Staining with Myc antibody shows weak signals in the regions of the antennae associated with basiconic sensilla, but strong signals in the trichoid/intermediate region. Together, trichoid and intermediate sensilla house a total of 10 olfactory neurons. I therefore examined the response of each OSN to its ligand to determine if a loss of *OS-E* and *OS-F* altered odorant sensitivity or response kinetics.

OS-E/F mutant OSNs show normal or increased spontaneous activity

The previously described OBP mutant *lush*^{1} shows a significant reduction in spontaneous activity of Or67d neurons[11]. I therefore hypothesized that mutants lacking *OS-E* and *OS-F* might also show altered spontaneous activity in the 10 OSNs found in *OS-E/F*-expressing sensilla[82].

None of the neurons showed a decrease in spontaneous activity. Surprisingly, two of the neurons showed a marked increase in spontaneous activity, which was rescued by transgenic expression of the *OS-E/F* gene region (Figure 4-1 A). Both neurons are found in the at4 sensillum, and express Or47b and Or88a respectively. Previous work has shown that the Or65abc neuron, while present, has a very low rate of spontaneous activity. To determine if the increase in small-amplitude spikes was from Or88a or Or65abc neurons, I used a double *Or47b;Or88a* mutant to look at Or65abc activity in isolation. The low spontaneous activity of these mutant sensilla confirmed that the increase in small-amplitude spikes is from Or88a-expressing neurons.

Mechanisms underlying increases in spontaneous activity

As previously noted, the OBP *lush* contributes to the spontaneous activity of Or67d neurons, where a loss of *lush* reduces spontaneous activity significantly. Conversely, loss of *SNMP1* causes an increase in Or67d spontaneous activity as an effect of environmental cVA exposure. Taking this into consideration, I tested the spontaneous activity of at4 neurons in flies reared in complete isolation from food sources and other flies by transferring single pupae to empty vials containing a water-soaked kimwipe. *OS-E/F* mutant flies still showed increased spontaneous activity. The increased spontaneous activity is rescued by transgenic expression of *OS-E/F*, but the cause of the increase remains unclear.

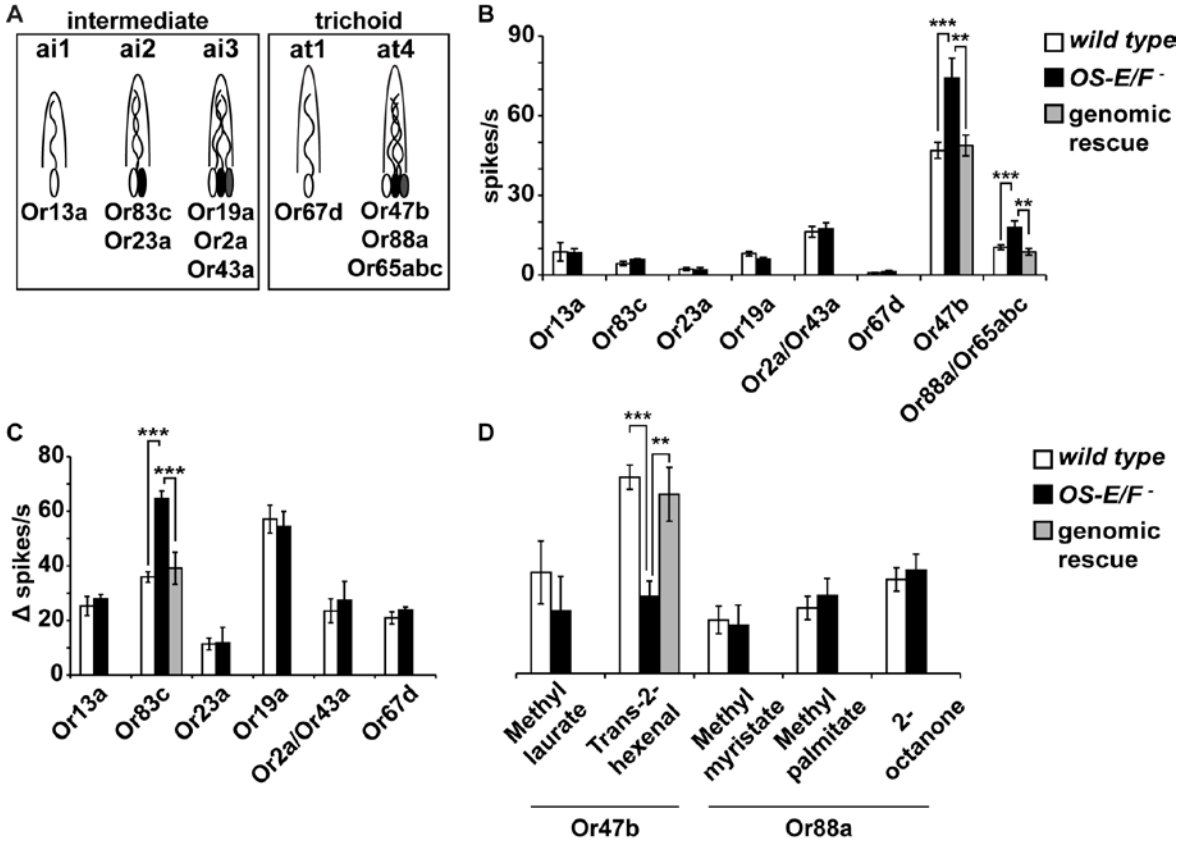

Figure 4-1. Spontaneous and evoked activity from wild type and *OS-E/F* mutants. A. Cartoon of two trichoid and three intermediate sensilla classes normally expressing *OS-E* and *OS-F*, depicting the neurons expressing the characteristic odorant receptors defining each neuron class. B. Average spontaneous activity of individual trichoid and intermediate neurons of the indicated genotypes in the absence of odorants. Or2a and Or43a as well as Or88a and Or65abc neuron responses were combined due to similarity in spike amplitudes. Or88a and Or65abc spontaneous rates were determined in the Or47b mutant[101]. C. Odor-induced responses of trichoid and intermediate neurons to the best known activating ligands for each neuron. n=5-10. D. Responses of at4 neurons to known ligands[24, 25]. All odorants were used at a 10% concentration. Error bars indicate SEM.

A subset of *OS-E/F* mutant OSNs show abnormal odorant sensitivity

I next examined the odorant tuning and sensitivity of each OSN using the best-known activator for each neuron. Most neurons did not show any change in sensitivity, but Or83c neurons showed an apparent increased sensitivity in the absence of *OS-E* and *OS-F* (Figure 4-1 C). Conversely, Or47b neurons appeared to have decreased sensitivity to the ligand trans-2-hexenal, though the responses to other known activators of Or47b were no affected (Figure 4-1 D). Both of these effects were reverted by transgenic expression of the *OS-E/F* gene region in an *OS-E/F* mutant background.

Apparent changes in odorant sensitivity result from a deactivation defect

Delta spikes/s calculates the change in activity that occurs in a single second following odorant presentation. Upon examining the traces for Or83c and Or47b neurons I found that the apparent changes in sensitivity were in fact the result of delayed deactivation. This deactivation defect is apparent when the trace is analyzed for the number of spikes occurring in a 1 second bin, for the duration of time that the recording is taken (Figure 4-2 A, B). Using this quantification I was also able to identify a deactivation defect in Or67d neurons—while the total number of spikes in the 10-11s bin is the same as wildtype, the number of spikes significantly increased in the subsequent seconds when *OS-E* and *OS-F* are absent (Figure 4-2 C).

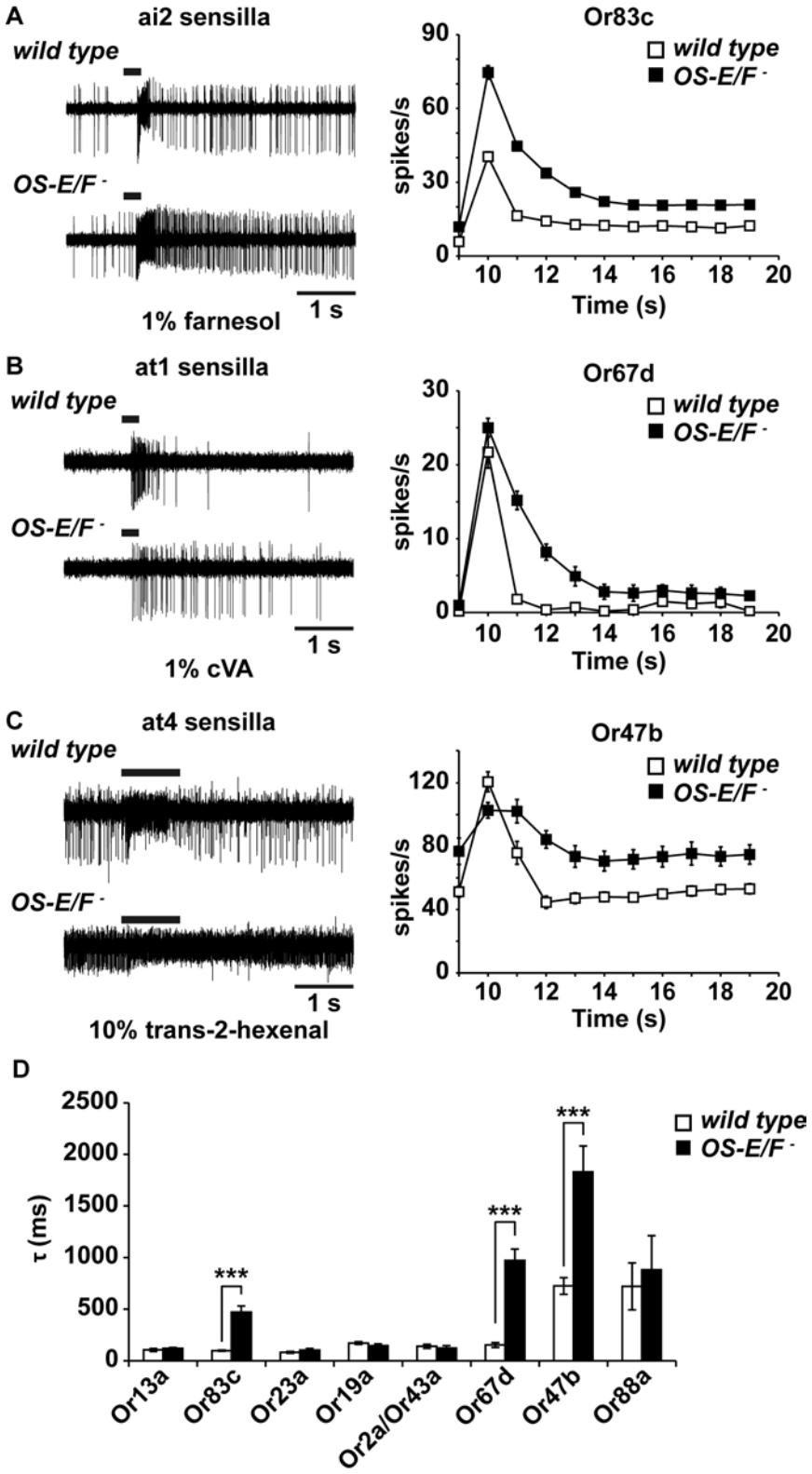
A
ai2 sensilla
wild type
OS-E/F -
1 s
1% farnesol
Or83c
wild type
OS-E/F -
spikes/s
Time (s)
B
at1 sensilla
wild type
OS-E/F -
1 s
1% cVA
Or67d
wild type
OS-E/F -
spikes/s
Time (s)
C
at4 sensilla
wild type
OS-E/F -
1 s
10% trans-2-hexenal
Or47b
wild type
OS-E/F -
spikes/s
Time (s)
D
τ (ms)
wild type
OS-E/F -
***
Or13a
Or83c
Or23a
Or19a
Or2a/Or43a
Or67d
Or47b
Or88a

Figure 4-2. Deactivation kinetics are abnormal to a subset of odorants in *OS-E/F* mutants. A. Comparison of mutant ai2a neuronal responses to farnesol. Left, representative 5-second traces for 1% farnesol. Right, time course of activation and deactivation as measured by binning spikes in 0.5-second bins. Note delayed return to baseline activity in the mutants. B. Comparison of wild type and *OS-E/F* mutant Or67d neurons to cVA. Left, representative traces, right, time course of activation and deactivation. C. Comparison of wild type and *OS-E/F* mutant at4 neuronal responses to trans-2-hexenal. Left, representative traces, right, time course of activation and deactivation. D. Time constant τ of deactivation of all tested olfactory neurons. n=10-20. Error bars indicate SEM.

I next sought to more precisely define the deactivation kinetics by analyzing the tau values for each trace. A trace was binned into 50ms intervals starting from time point 10s, when odorant is presented. The total number of spikes was counted from 10s to 20s. The resulting data was plotted as an exponential decay curve from which tau could be calculated. Essentially, calculating the tau of each trace indicates the time point, in milliseconds, at which neuronal activity reaches the natural log (~37%) of its peak value. I calculated the τ values of all previously tested neurons, and found that only Or83c, Or67d, and Or47b showed a deactivation defect (Figure 4-2 D).

The *OS-E/F* deactivation defect is dose-independent and odorant specific

Or83c in particular is exquisitely sensitive to farnesol, and is activated by concentrations as low as 0.001%[20]. Since I initially used 1% farnesol to screen for odorant responses, it is possible that the phenotype results from saturating the neuron. I therefore examined the kinetics of deactivation at lower doses. In my hands, 0.01% farnesol is the lowest dilution on filter paper that is capable of activating Or83c neurons (Figure 4-3 A). The deactivation defect is still observable at these low doses (Figure 4-3 B). This result suggests that the deactivation defect is not a result of the neuron being overstimulated by high concentrations of odor.

Only a subset of OSNs show delayed deactivation kinetics when *OS-E* and *OS-F* are absent. This could indicate that these neurons exclusively require *OS-E* and *OS-F*, or that they are required only for specific receptors. Or67d neurons are exclusively tuned to cVA, and no other potent activating ligands have been identified. Or83c neurons are potently activated by

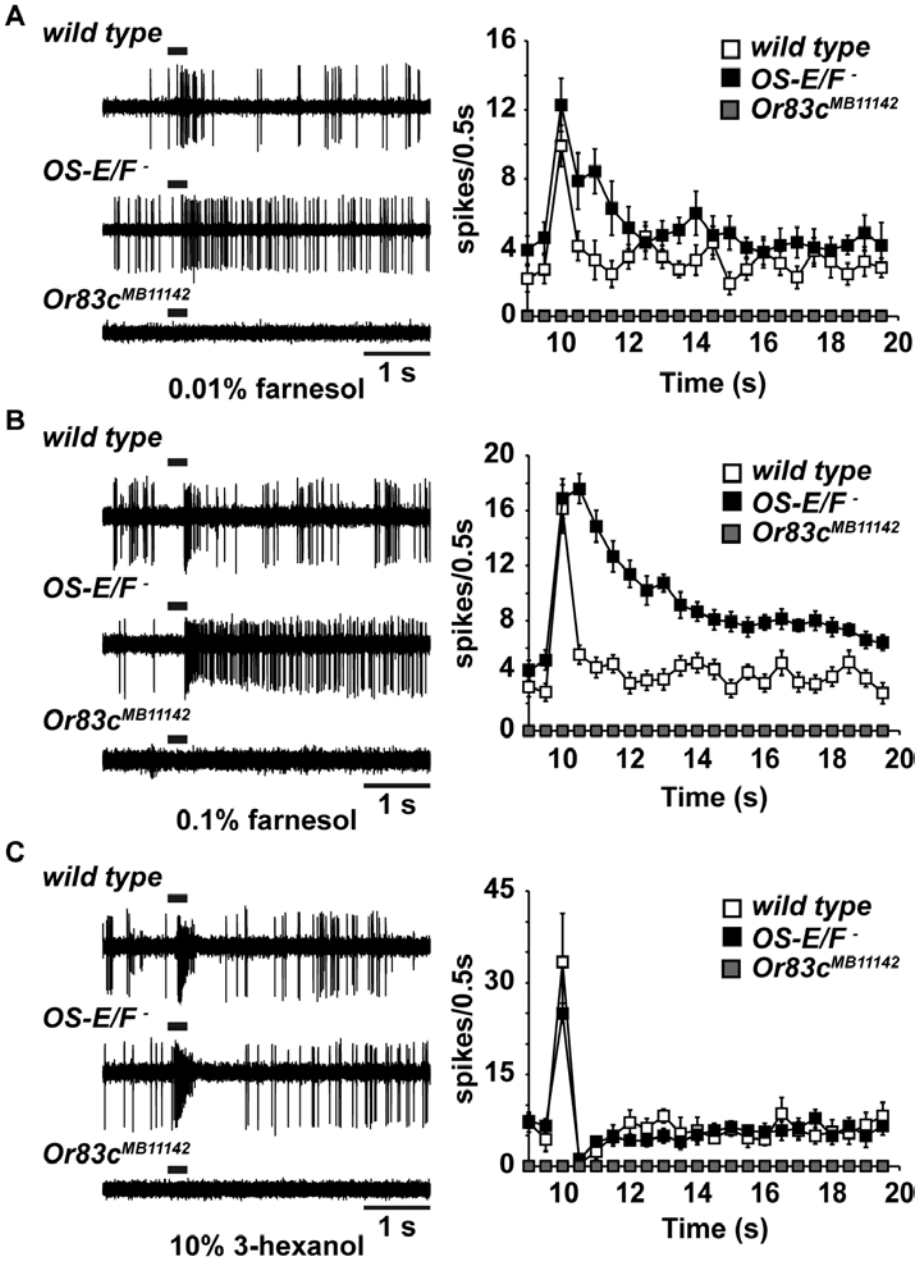

Figure 4-3. Odorant specificity of the Or83c deactivation defect. A. Responses of Or83c neurons from wild type, OS-E/F mutant and Or83c mutants in response to 0.01% farnesol. Left, representative 5-second traces, right, time course of responses assayed by binning spikes in 500 millisecond bins. B. Responses of wild type, OS-E/F mutants and Or83c mutants to 0.1% farnesol. Despite lower peak activation, a prominent deactivation defect is still present in the mutants. C. Responses of wild type, OS- E/F mutants and Or83c mutants to 10% 3-hexanol. No differences in deactivation are apparent between wild type and OS-E/F mutants. Or83c mutants do not respond to 3-hexanol. n < 5 flies per genotype. Error bars represent SEM.

farnesol, but can also be stimulated by high doses of 3-hexanol[20]. To determine if the deactivation defect is odorant-specific, I applied 10% 3-hexanol to Or83c neurons in both wild type and *OS-E/F* mutant flies. Surprisingly, mutant neurons stimulated with 10% 3-hexanol do not show a deactivation defect, indicating that this phenotype is odorant-specific (Figure 4-3 C). To confirm that this response is indeed mediated by Or83c neurons, I repeated the experiment with an Or83c null mutant[20]. There was no change in the response to 3-hexanol confirming that the observed response is due to Or83c OSN activation.

Latency is not affected in *OS-E/F* mutants

The *OS-E/F* mutant deactivation defect might indicate a role for these OBPs in odorant clearance from the sensillum lymph. If rapid clearance cannot occur, the ligand may bind repeatedly to the receptor complex, causing prolonged activation of the neuron. In this model, OS-E/F and the receptor complex are competing for the binding of odorant molecules in the sensillum lymph. If this model is true, it is likely that the OBPs are capable of binding some molecules before they reach the receptor, resulting in a slight latency to response. Therefore, an *OS-E/F* mutant would show a decrease in latency since odorant molecules are free to move to the receptor. I analyzed the latency of the responses of Or83c and Or67d neurons to low doses of their respective ligands.

Latency is calculated as the time from trigger activation of the valve initiating the flow of odorant to the preparation, to arrival of the odorant molecules to the receptors, producing a

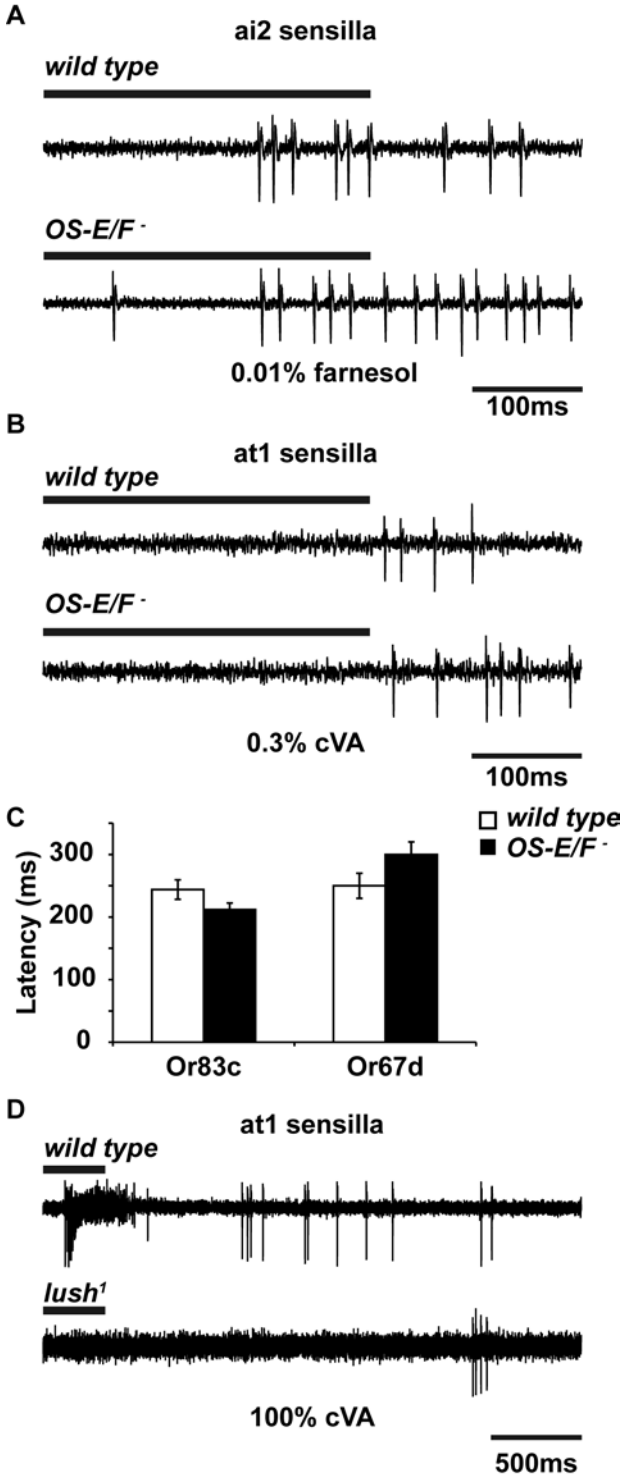
A
ai2 sensilla
wild type
OS-E/F -
0.01% farnesol
100ms
B
at1 sensilla
wild type
OS-E/F -
0.3% cVA
100ms
C
wild type
OS-E/F -
Latency (ms)
300
200
100
0
Or83c
Or67d
D
at1 sensilla
wild type
lush1
100% cVA
500ms

Figure 4-4. Activation kinetics for farnesol and cVA are not affected by loss of *OS-E* and *OS-F*. A. Representative 500 millisecond traces from wild type and *OS-E/F* mutant ai2 sensilla to 0.01% farnesol. B. Representative 3 second traces from wild type, *OS-E/F* mutant, and lush1 Or67d neurons to 0.3% cVA. C. Analysis of latency to activation for neurons and genotypes indicated. D. Representative 2.5 second traces from wild type and *lush* mutant sensilla to 100% cVA.

cluster of spikes. Both Or83c and Or67d neurons show near-identical activation latency, indicating that *OS-E* and *OS-F* function exclusively in the removal of ligand from the receptor after neuronal activation (Figure 4-4 A, B). In comparison, a *lush*^{1} mutant stimulated with 100% cVA does not show activation for nearly 2 seconds following odorant presentation (Figure 4-4 C).

Or47b neurons have high spontaneous activity, making it difficult to identify when a cluster of spikes is elicited specifically by odorant presentation. For Or47b neurons I therefore examined the 50ms bins used to calculate τ, and found that there is no difference between wild type and *OS-E/F* mutants.

Latency to first spike vs. latency to peak activation

I initially measured latency as the time until a cluster of spikes occurred, presumably in response to odorant presentation. While the time until first odorant-elicited spikes occurs is easily measured through examination of the trace, the latency to peak activation requires quantification of 50ms bins to define "peak activation." In Or67d neurons the peak activation of OS-E/F mutants is shifted to the right by one 50ms bin (Figure 4-5 B). The total number of spikes in this bin is also significantly decreased from the wild type. This could indicate delayed dissociation of odorant molecules from the receptor complex.

Mutant Or47b neurons show a significant decrease in the number of spikes constituting peak activation (Figure 4-5 C). This is likely an effect of the increase in spontaneous activity—since the neuron is already significantly more active, it likely reaches its saturation point when odorant is applied.

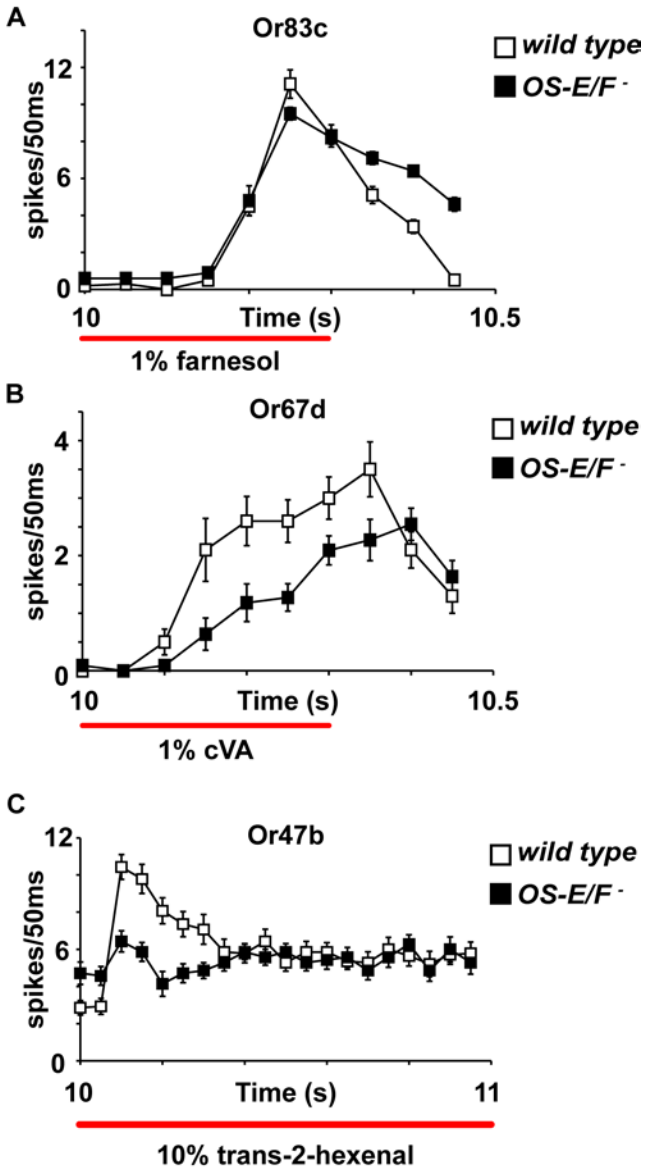

Figure 4-5. Peak activation in *OS-E/F* mutants. A. Time course of Or83c activation. Red bar denotes the 300ms when 1% farnesol is applied. B. Time course of Or67d activation. Red bar denotes the 300ms when 1% cVA is applied. C. Time course of Or47b activation. The red bar denotes the 1000ms when 10% trans-2-hexenal was applied.

No genetic interaction of *SNMP1* and *OS-E/F*

Previous work from the Smith lab shows that deactivation defects in Or67d and Or83c are also found in *SNMP1* mutants[20]. I wanted to determine if there was a genetic interaction between *SNMP1* and *OS-E/F* in the deactivation of Or83c neurons after farnesol exposure. I first compared the τ values of *SNMP1* and *OS-E/F* mutants to 100% farnesol separately (Figure 4-6 A, B). I then generated a double mutant in which the *SNMP1* mutant was recombined into the *OS-E/F* mutant background, and tested the response. The *OS-E/F* mutant deactivation defect is significantly stronger than the *SNMP1* mutant defect. Combining the *SNMP1* and *OS-E/F* mutant gives a deactivation defect approximately equal to the value in the *OS-E/F* mutant alone (Figure 4-6 A, B). An additive effect would indicate that these genes function in separate mechanisms of deactivation. Since no additive effect occurred, it is likely that these genes function in the same pathway. *OS-E* and *OS-F* are specific to deactivation, so it is possible that SNMP interacts with these OBPs to facilitate rapid removal of odorants from the receptor complex.

***OS-E* and *OS-F* are functionally redundant for rapid deactivation**

In initial experiments I used a transgene to express 10.6kb of the *OS-E/F* gene region in the *OS-E/F* mutant background. This transgene was sufficient to restore wild type deactivation kinetics, demonstrating the requirement of *OS-E* and *OS-F* for rapid deactivation. I wondered if

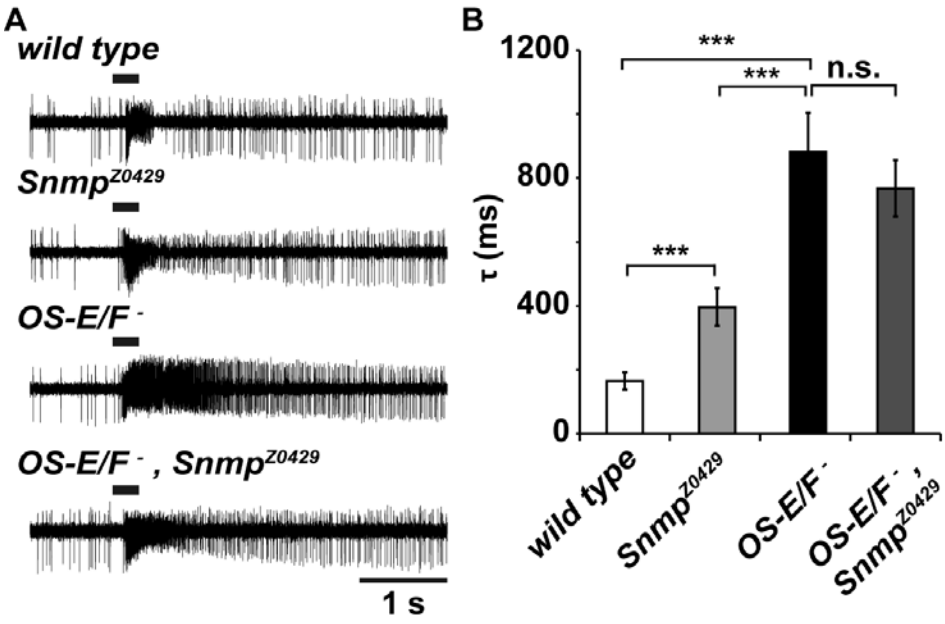

Figure 4-6. *OS-E/F* mutants show a stronger deactivation defect than *SNMP* mutants. A. Representative 5 second traces from wild type, *SNMP*^{Z0429}, *OS-E/F* mutant, and *OS-E/F* mutant, *SNMP*^{Z0429} double mutant ai2 sensilla to 100% farnesol. B. Deactivation time constant (τ) for all genotypes tested. n = 5. Error bars indicate SEM.

both genes were required, or if each mediated responses to separate odorants. I therefore mutated the transgenic sequence to remove the coding region of either *OS-E* or *OS-F*, and expressed these modified transgenes in the null mutant background (Figure 4-7 A). Expression of either *OS-E* or *OS-F* was sufficient to restore rapid deactivation in all affected neurons (Figure 4-7 B). *OS-E* and *OS-F* are therefore functionally redundant for deactivation.

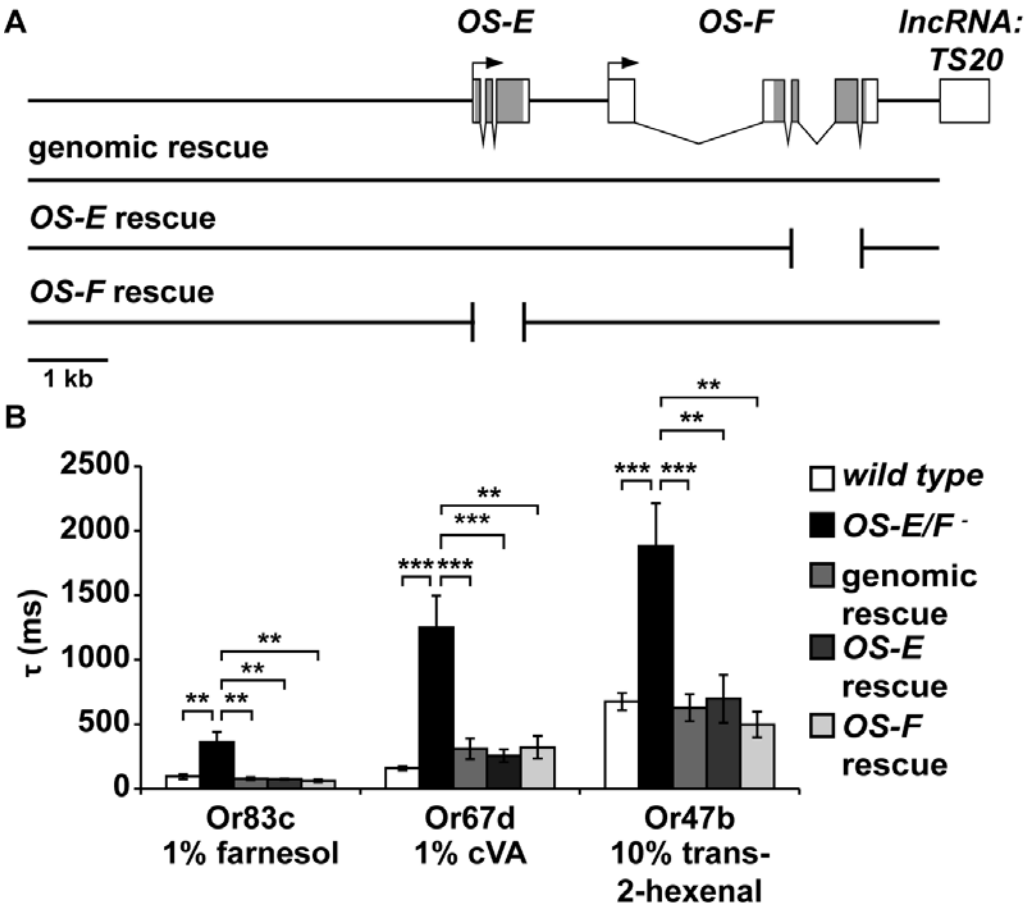

Figure 4-7. *OS-E* and *OS-F* are functionally redundant for rapid neuronal deactivation. A. Map of the *OS-E/F* gene region with shaded regions to indicate coding regions. The lines directly beneath the map depict the regions that were used to evaluate the function of individual OBP genes. Breaks in the lines showing individual rescues show where the coding region of either *OS-E* or *OS-F* was excised from the genomic rescue construct (see Materials and Methods for details). B. Time constants of deactivation for Or83c, Or47b and Or67d neurons with the genotypes indicated. Delayed deactivation present in the *OS-E/F* mutants is reversed by all forms of the rescuing transgene. n=5-10. Error bars indicate SEM.

CHAPTER FIVE
Conclusions and Recommendations

OS-E and *OS-F* function in the rapid deactivation of a subset of olfactory neurons

OBPs comprise a large, diverse family of proteins that are largely uncharacterized. The *Drosophila* OBPs that have been functionally described adopt numerous different roles in the olfactory system—as transporters, sensitizers, buffers, or selective blockers of neuronal activity. It is worth noting that these functions precede activation of the odorant receptor complex. The original proposed role of OBPs was in the rapid clearance of odorant molecules from the receptor complex or sensillum lymph, thereby allowing the neuron to maintain its sensitivity.

Here, I have generated a unique mutant for the *OS-E/F* gene region that encompasses two highly similar co-expressed OBPs. Mutants lacking *OS-E* and *OS-F* show a delayed deactivation in a subset of odorant receptors to specific odorants: farnesol detected by Or83c, cVA detected by Or67d, and trans-2-hexenal detected by Or47b.

How specific are the interactions between these activating odorants and *OS-E/F*? While Or67d is exclusively tuned to cVA, Or83c can be activated by other odorants. I find that the deactivation defect is only present in Or83c neurons when farnesol is used. I verified that this interaction is Or83c-specific by using an Or83c mutant fly that is not activated by farnesol or any other known Or83c activators.

OS-E and *OS-F* are functionally redundant OBPs

OS-E and *OS-F* are less than 1kb apart on the third *Drosophila* chromosome and are likely the result of recent gene duplication. This high level of similarity, and the fact that *OS-E* and *OS-F* are always co-expressed, strongly suggested a redundancy of function. I have found that either *OS-E* or *OS-F* alone is sufficient to restore the rapid deactivation of olfactory neurons in response to their ligands.

A proposed model for OS-E/F function

How do OS-E and OS-F facilitate rapid deactivation of olfactory neurons? I have demonstrated that a loss of *OS-E/F* does not broadly affect latency to activation, indicating that these OBPs do not simply compete with the receptor complex for binding of odorants. Little is known about the interactions between OBPs and odorant receptors, since these are likely transient events lasting in the range of milliseconds. I propose a model for OS-E/F function in which a subset of odorants does not readily dissociate from the receptor complex. OS-E and OS-F may "pull" these odorants off the receptors to facilitate rapid deactivation (Figure 5-1). When OS-E and OS-F are absent, the molecules dissociate at a significantly slower rate, prolonging the activation of the neuron.

The involvement of *SNMP1* in deactivation of Or83c and Or67d neurons offers a potential clue to the mechanism of odorant dissociation. In the absence of *SNMP1*, cVA essentially becomes "stuck" to the receptor complex, leading to prolonged activation of the neuron. Deactivation of Or83c neurons to farnesol is also significantly delayed in *SNMP1* mutants, suggesting that these molecules may also become "stuck" to the complex, though the extent to which these molecules

remain bound has not been studied. It is not known how *SNMP1* facilitates removal of odorant molecules from the receptor complex, though it is hypothesized that *SNMP1* somehow lowers the energy barrier to dissociation. The *OS-E/F* mutant shows a much stronger deactivation defect in Or83c neurons than *SNMP1* mutants, while *SNMP1* mutants have the stronger defect in Or67d neurons. When I combined the *OS-E/F* mutant and *SNMP1* mutant and examined Or83c deactivation, it was not significantly different from the defect seen in *OS-E/F* mutants alone. Since the two mutations do not have an additive effect, they likely function in the same deactivation pathway. SNMP1 is a membrane-bound protein and is therefore more likely to encounter odorant molecules before OS-E and OS-F.

Future experiments

How does rapid deactivation of an olfactory neuron function in *Drosophila* behavior? The ability of the fly to maintain its sensitivity to odorant is critical for finding food sources and mates. It is possible that an *OS-E/F* mutant fly would show impaired chemotaxis when moving up a concentration gradient. The lack of *OS-E* and *OS-F* could lead to an accumulation of odorant molecules in the sensillum lymph, making it difficult for the fly to detect changes in odorant concentration. Other possibilities include effects on social interactions, though in preliminary courtship assays I did not observe any significant changes.

Resolution of the structure of OS-E or OS-F proteins bound to odorants of interest would also provide insight into their function. Like other OBPs, OS-E and OS-F presumably comprise a six alpha-helix structure surrounding a hydrophobic binding pocket. There may be a

conformational change similar that of cVA-bound LUSH, that is critical for the appropriate function of these OBPs. Mutating the binding pocket, for example, could interfere with the ability of the OBP to bind its ligand and clear it from the odorant receptor. Similarly, the experiments used to determine OBP49a's function might offer similar insights. If a membrane-tethered OS-E or OS-F is sufficient to restore rapid deactivation, then we may be able to infer a more direct interaction between these OBPs and the odorant receptor complex.

Summary

In summary, I have generated a novel mutant for two *Drosophila* OBPs, *OS-E* and *OS-F*. Loss of these OBPs exclusively affects the deactivation kinetics of a subset of olfactory neurons. I furthermore showed that these deactivation defects are dose-independent and odorant-specific, and that *OS-E* and *OS-F* are functionally redundant for deactivation. Prior to this, no OBP had been definitively demonstrated to function in the deactivation of odorant responses. This expands our understanding of the roles of OBPs in insect olfaction.

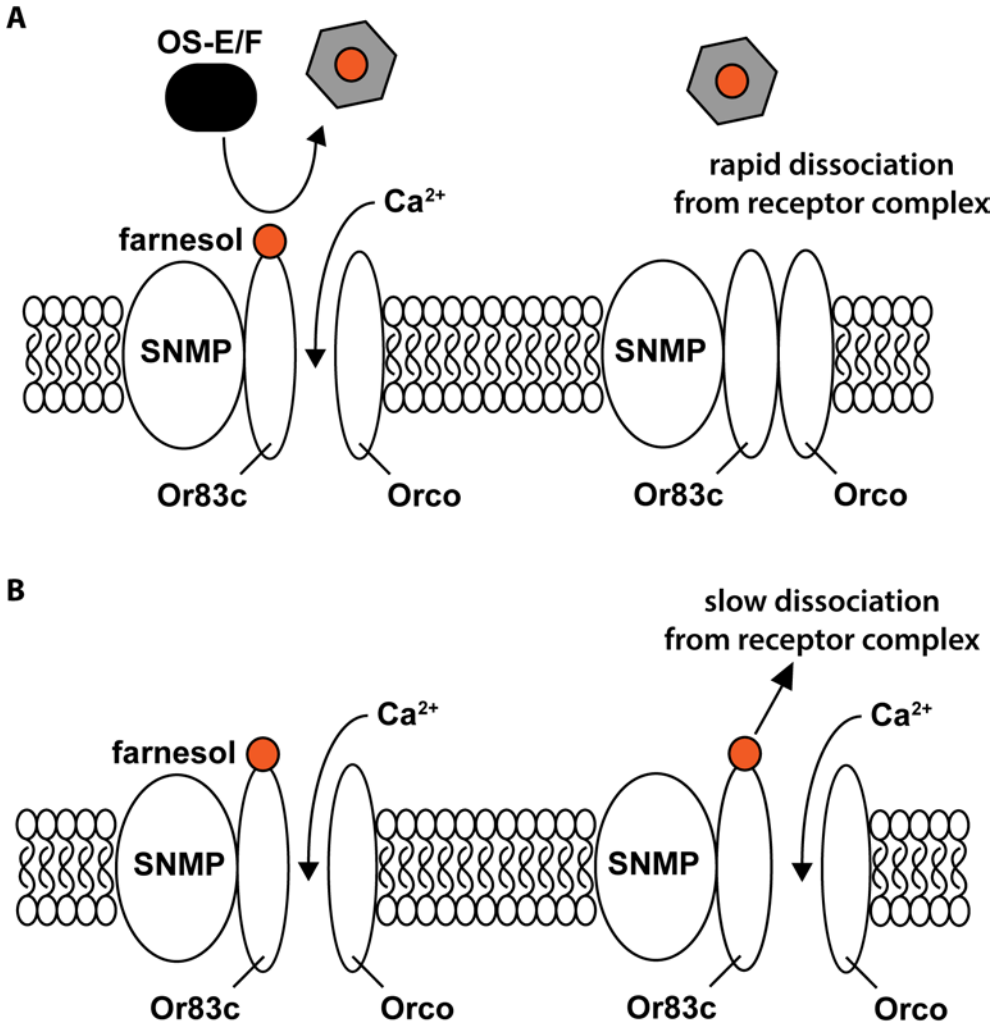

Figure 5-1. A proposed model for OS-E/F function in deactivation. A. When OS-E and OS-F are present; they facilitate the rapid removal of a farnesol molecule from the Or83c receptor complex, allowing the neuron to deactivate. B. In the absence of OS-E and OS-F, a farnesol molecule dissociates slowly from the Or83c receptor complex, delaying deactivation of the neuron.

APPENDIX A
RTPCR Verification of OS-E/F Mutant

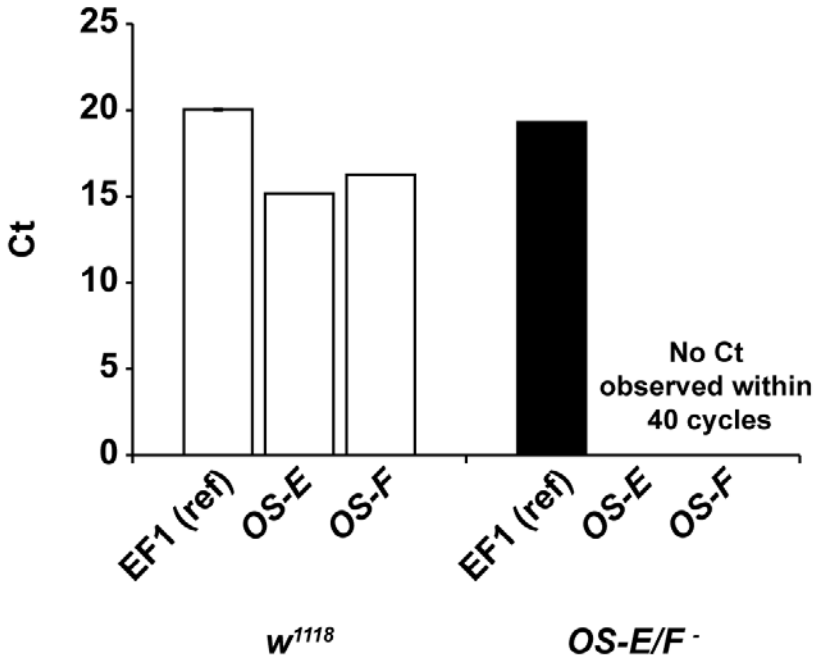

APPENDIX B
Expression of Myc-tagged *OS-E*

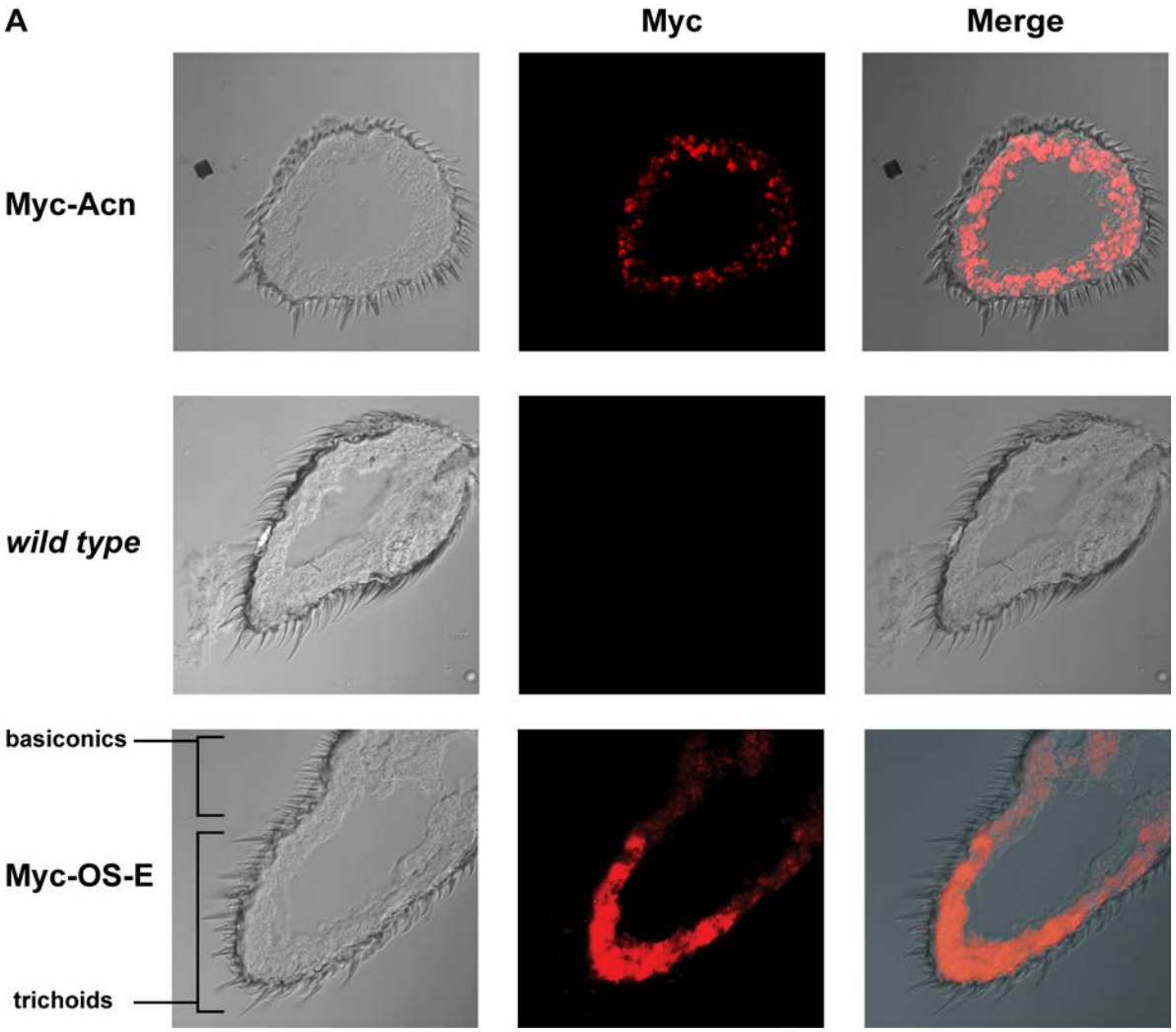

10µm sections through the antennae of flies of the genotypes indicated. Sections were stained with a Myc antibody. Regions associated with specific sensillum types are indicated.

APPENDIX C
Electrophysiology Data and Statistics

Figure 4-1 B

Neuron	Spontaneous activity (spikes/s)			p value		
	Wild type	*OS-E/F*$^{--}$	*OS-E/F* rescue	*Wild type* to mutant	*Wild type* to rescue	Mutant to rescue
Or13a	8.72 ± 3.5	8.46 ± 1.4		0.922		
Or83c	4.34 ± 0.8	5.82 ± 0.4		0.207		
Or23a	2.24 ± 0.6	2 ± 0.9		0.839		
Or19a	8.10 ± 0.8	6.01 ± 0.7		0.109		
Or2a/Or43a	16.2 ± 2.1	17.4 ± 2.3		0.723		
Or67d	0.8 ± 0.19	1.16 ± 0.47		0.499		
Or47b	46.9 ± 3.00	74.3 ± 7.42	48.8 ± 3.9	2.89×10^{-4}	0.43	0.025
Or88a/ Or65abc	10.47 ± 0.97	17.86 ± 2.51	8.76 ± 1.3	7.35×10^{-5}	0.29	1.12×10^{-3}

Figure 4-1 C-D

Neuron	Odorant	Odorant-evoked activity (Δ spikes/s)			p value		
		Wild type	*OS-E/F*$^{-}$	*OS-E/F* rescue	*Wild type* to mutant	*Wild type* to rescue	Mutant to rescue
Or13a	10% 1-octen-3-ol	25.3 ± 3.5	27.9 ± 1.6		0.51		
Or83c	1% farnesol	35.9 ± 1.9	64.6 ± 2.8	39.1 ± 5.9	1.15×10^{-7}	0.28	1.76×10^{-4}
Or23a	10% cyclohexanone	11.4 ± 2.1	11.8 ± 5.7		0.94		
Or19a	1% limonene	57.1 ± 5.1	54.5 ± 5.4		0.75		
Or2a/ Or43a	10% benzaldehyde	23.5 ± 4.4	27.3 ± 6.9		0.63		
Or67d	1% cVA	20.9 ± 2.2	23.8 ± 1.0		0.23		
Or47b							
	10% trans-2-hexenal	72.4 ± 4.5	28.5 ± 5.7		3.21×10^{-6}		
	10% methyl laurate	37.3 ± 11.6	23.2 ± 12.6		0.43		
Or88a/ Or65abc							

	10% 2-octanone	34.7 ± 4.3	38.1 ± 6	66.1 ± 9.9	0.29	0.51	0.003
	10% methyl myristate	19.8 ± 5.0	17.8 ± 7.5		0.83		
	10% methyl palmitate	24.2 ± 4.3	28.7 ± 6.3		0.57		

Figure 4-2 D

Neuron	τ (ms)		p value
	Wild type	*OS-E/F⁻*	
Or13a	106.1 ± 14.5	121.4 ± 6.6	0.37
Or83c	99.2 ± 4.6	472.1 ± 58.2	5.14×10^{-6}
Or23a	83.2 ± 7.9	104.7 ± 14.3	0.23
Or19a	171.9 ± 13.1	148.5 ± 17.0	0.31
Or2a/Or43a	140.9 ± 19.5	123.9 ± 24.8	0.60
Or67d	153.7 ± 22.4	971.7 ± 112.5	1.69×10^{-6}
Or47b	725.7 ± 81.0	1830 ± 250.8	6.95×10^{-6}
Or88a/Or65abc	720.9 ± 227.6	882.1 ± 330.0	0.46

Figure 4-3 A-C

Odorant	τ (ms)		p value
	Wild type	*OS-E/⁻*	
0.01% farnesol	106.4 ± 18.9	905.6 ± 267.3	0.002
0.1% farnesol	109.4 ± 42.2	870.48 ± 152.7	0.001
10% 3-hexanol	109.6 ± 32.9	115.2 ± 14.5	0.87

Figure 4-4 C

Neuron	Odorant	Latency (ms)		p value
		Wild type	*OS-E/⁻*	
Or83c	0.01% farnesol	243.8 ± 15.6	211.9 ± 10.5	0.15
Or67d	0.3% cVA	249.9 ± 20.0	299.9 ± 20.2	0.12

Figure 4-6 B

τ (ms)			
Wild type	*SNMP⁻*	*OS-E/F⁻*	Double mutant
165.2 ± 27.1	396.7 ± 58.9	882.3 ± 121.9	768.3 ± 88.6

p value					
Wild type to *SNMP*$^{-}$	*Wild type* to *OS-E/F*$^{-}$	*Wild type* to double mutant	*SNMP*$^{-}$ to *OS-E/F*$^{-}$	*SNMP*$^{-}$ to double mutant	*OS-E/F*$^{--}$ to double mutant
0.003	9.27×10^{-3}	2.91×10^{-5}	0.006	0.006	0.46

Figure 4-7 B

Neuron	Odorant	τ (ms)				
		Wild type	*OS-E/F*$^{-}$	*OS-E/F* rescue	*OS-E* rescue	*OS-F* rescue
Or83c	1% farnesol	96.4 ± 19.2	364.3 ± 76.8	80.9 ± 12.0	76.5 ± 4.2	63.8 ± 9.5
Or67d	1% cvA	160.7 ± 17.2	1249.6 ± 246.6	310.4 ± 80.3	257.5 ± 50.1	322.2 ± 88.7
Or47b	10% trans-2-hexenal	676.4 ± 67.2	1882.5 ± 328.9	629.1 ± 102.7	699.2 ± 184.7	499.1 ± 99.4

Genotypes	p value		
	Or83c	Or67d	Or47b
Wild type to *OS-E/F*$^{-}$	1.3×10^{-3}	9.8×10^{-5}	2.55x10-4
Wild type to *OS-E/F* rescue	0.99	0.99	0.70
Wild type to *OS-E* rescue	0.99	0.99	0.90
Wild type to *OS-F* rescue	0.99	0.99	0.14
OS-E/F^{-} to *OS-E/F* rescue	0.001	0.0019	3.79×10^{-4}
OS-E/F- to *OS-E* rescue	1.3×10^{-3}	1.6×10^{-3}	4.8×10^{-3}
OS-E/F- to *OS-F* rescue	0.003	1.3×10^{-3}	1.23×10^{-3}
OS-E/F rescue to *OS-E* rescue	0.99	0.99	0.73
OS-E/F rescue to *OS-F* rescue	0.99	0.99	0.40
OS-E rescue to *OS-F* rescue	0.99	0.99	0.39

BIBLIOGRAPHY

1. McBride CS, Baier F, Omondi AB, Spitzer SA, Lutomiah J, Sang R, Ignell R, Vosshall LB. Evolution of mosquito preference for humans linked to an odorant receptor. Nature. 2014;515(7526):222-7. doi: 10.1038/nature13964. PubMed PMID: 25391959; PMCID: PMC4286346.
2. McMeniman CJ, Corfas RA, Matthews BJ, Ritchie SA, Vosshall LB. Multimodal integration of carbon dioxide and other sensory cues drives mosquito attraction to humans. Cell. 2014;156(5):1060-71. doi: 10.1016/j.cell.2013.12.044. PubMed PMID: 24581501; PMCID: PMC4007582.
3. Mansouri A, Cregut M, Abbes C, Durand MJ, Landoulsi A, Thouand G. The Environmental Issues of DDT Pollution and Bioremediation: a Multidisciplinary Review. Appl Biochem Biotechnol. 2017;181(1):309-39. doi: 10.1007/s12010-016-2214-5. PubMed PMID: 27591882.
4. Fairbrother A, Purdy J, Anderson T, Fell R. Risks of neonicotinoid insecticides to honeybees. Environ Toxicol Chem. 2014;33(4):719-31. doi: 10.1002/etc.2527. PubMed PMID: 24692231; PMCID: PMC4312970.
5. Venthur H, Zhou JJ. Odorant Receptors and Odorant-Binding Proteins as Insect Pest Control Targets: A Comparative Analysis. Front Physiol. 2018;9:1163. doi: 10.3389/fphys.2018.01163. PubMed PMID: 30197600; PMCID: PMC6117247.
6. Lee Y, Kim SH, Montell C. Avoiding DEET through insect gustatory receptors. Neuron. 2010;67(4):555-61. doi: 10.1016/j.neuron.2010.07.006. PubMed PMID: 20797533; PMCID: PMC2929391.
7. Dennis EJ, Goldman OV, Vosshall LB. Aedes aegypti Mosquitoes Use Their Legs to Sense DEET on Contact. Curr Biol. 2019;29(9):1551-6 e5. doi: 10.1016/j.cub.2019.04.004. PubMed PMID: 31031114; PMCID: PMC6504582.
8. Oliveira DS, Brito NF, Franco TA, Moreira MF, Leal WS, Melo ACA. Functional Characterization of Odorant Binding Protein 27 (RproOBP27) From Rhodnius prolixus Antennae. Front Physiol. 2018;9:1175. doi: 10.3389/fphys.2018.01175. PubMed PMID: 30210359; PMCID: PMC6119777.
9. Zhang XY, Zhu XQ, Gu SH, Zhou YL, Wang SY, Zhang YJ, Guo YY. Silencing of odorant binding protein gene AlinOBP4 by RNAi induces declining electrophysiological responses of Adelphocoris lineolatus to six semiochemicals. Insect Sci. 2017;24(5):789-97. doi: 10.1111/1744-7917.12365. PubMed PMID: 27265520.
10. Antony B, Johny J, Aldosari SA. Silencing the Odorant Binding Protein RferOBP1768 Reduces the Strong Preference of Palm Weevil for the Major Aggregation Pheromone Compound Ferrugineol. Front Physiol. 2018;9:252. doi: 10.3389/fphys.2018.00252. PubMed PMID: 29618982; PMCID: PMC5871713.
11. Xu P, Atkinson R, Jones DN, Smith DP. Drosophila OBP LUSH is required for activity of pheromone-sensitive neurons. Neuron. 2005;45(2):193-200. doi: 10.1016/j.neuron.2004.12.031. PubMed PMID: 15664171.
12. S.R Shanbhag BM, R.A Steinbrecht. Atlas of olfactory organs of Drosophila melanogaster: 1. Types, external organization, innervation and distribution of olfactory sensilla.

International Journal of Insect Morphology and Embryology. 1999;28(4):377-97. doi: https://doi.org/10.1016/S0020-7322(99)00039-2.
13. Shanbhag SR, Muller B, Steinbrecht RA. Atlas of olfactory organs of Drosophila melanogaster 2. Internal organization and cellular architecture of olfactory sensilla. Arthropod Struct Dev. 2000;29(3):211-29. PubMed PMID: 18088928.
14. Steinbrecht RA, Muller B. On the stimulus conducting structures in insect olfactory receptors. Z Zellforsch Mikrosk Anat. 1971;117(4):570-5. PubMed PMID: 5088155.
15. Clyne P, Grant A, O'Connell R, Carlson JR. Odorant response of individual sensilla on the Drosophila antenna. Invert Neurosci. 1997;3(2-3):127-35. PubMed PMID: 9783438.
16. Couto A, Alenius M, Dickson BJ. Molecular, anatomical, and functional organization of the Drosophila olfactory system. Curr Biol. 2005;15(17):1535-47. doi: 10.1016/j.cub.2005.07.034. PubMed PMID: 16139208.
17. Hallem EA, Carlson JR. Coding of odors by a receptor repertoire. Cell. 2006;125(1):143-60. doi: 10.1016/j.cell.2006.01.050. PubMed PMID: 16615896.
18. Suh GS, Wong AM, Hergarden AC, Wang JW, Simon AF, Benzer S, Axel R, Anderson DJ. A single population of olfactory sensory neurons mediates an innate avoidance behaviour in Drosophila. Nature. 2004;431(7010):854-9. doi: 10.1038/nature02980. PubMed PMID: 15372051.
19. Hallem EA, Ho MG, Carlson JR. The molecular basis of odor coding in the Drosophila antenna. Cell. 2004;117(7):965-79. doi: 10.1016/j.cell.2004.05.012. PubMed PMID: 15210116.
20. Ronderos DS, Lin CC, Potter CJ, Smith DP. Farnesol-detecting olfactory neurons in Drosophila. J Neurosci. 2014;34(11):3959-68. doi: 10.1523/JNEUROSCI.4582-13.2014. PubMed PMID: 24623773; PMCID: PMC3951695.
21. Kaissling KE. Pheromone Reception in Insects: The Example of Silk Moths. In: Mucignat-Caretta C, editor. Neurobiology of Chemical Communication. Boca Raton (FL)2014.
22. Lin CC, Potter CJ. Re-Classification of Drosophila melanogaster Trichoid and Intermediate Sensilla Using Fluorescence-Guided Single Sensillum Recording. PLoS One. 2015;10(10):e0139675. doi: 10.1371/journal.pone.0139675. PubMed PMID: 26431203; PMCID: PMC4592000.
23. Ha TS, Smith DP. A pheromone receptor mediates 11-cis-vaccenyl acetate-induced responses in Drosophila. J Neurosci. 2006;26(34):8727-33. doi: 10.1523/JNEUROSCI.0876-06.2006. PubMed PMID: 16928861.
24. Dweck HK, Ebrahim SA, Thoma M, Mohamed AA, Keesey IW, Trona F, Lavista-Llanos S, Svatos A, Sachse S, Knaden M, Hansson BS. Pheromones mediating copulation and attraction in Drosophila. Proc Natl Acad Sci U S A. 2015;112(21):E2829-35. doi: 10.1073/pnas.1504527112. PubMed PMID: 25964351; PMCID: PMC4450379.
25. Pitts S, Pelser E, Meeks J, Smith D. Odorant Responses and Courtship Behaviors Influenced by at4 Neurons in Drosophila. PLoS One. 2016;11(9):e0162761. doi: 10.1371/journal.pone.0162761. PubMed PMID: 27617442; PMCID: PMC5019410.
26. van der Goes van Naters W, Carlson JR. Receptors and neurons for fly odors in Drosophila. Curr Biol. 2007;17(7):606-12. doi: 10.1016/j.cub.2007.02.043. PubMed PMID: 17363256; PMCID: PMC1876700.

27. Dweck HK, Ebrahim SA, Kromann S, Bown D, Hillbur Y, Sachse S, Hansson BS, Stensmyr MC. Olfactory preference for egg laying on citrus substrates in Drosophila. Curr Biol. 2013;23(24):2472-80. doi: 10.1016/j.cub.2013.10.047. PubMed PMID: 24316206.
28. Enjin A, Zaharieva EE, Frank DD, Mansourian S, Suh GS, Gallio M, Stensmyr MC. Humidity Sensing in Drosophila. Curr Biol. 2016;26(10):1352-8. doi: 10.1016/j.cub.2016.03.049. PubMed PMID: 27161501; PMCID: PMC5305172.
29. Benton R, Vannice KS, Gomez-Diaz C, Vosshall LB. Variant ionotropic glutamate receptors as chemosensory receptors in Drosophila. Cell. 2009;136(1):149-62. doi: 10.1016/j.cell.2008.12.001. PubMed PMID: 19135896; PMCID: PMC2709536.
30. Ai M, Min S, Grosjean Y, Leblanc C, Bell R, Benton R, Suh GS. Acid sensing by the Drosophila olfactory system. Nature. 2010;468(7324):691-5. doi: 10.1038/nature09537. PubMed PMID: 21085119; PMCID: PMC3105465.
31. Yao CA, Ignell R, Carlson JR. Chemosensory coding by neurons in the coeloconic sensilla of the Drosophila antenna. J Neurosci. 2005;25(37):8359-67. doi: 10.1523/JNEUROSCI.2432-05.2005. PubMed PMID: 16162917.
32. Clyne PJ, Warr CG, Freeman MR, Lessing D, Kim J, Carlson JR. A novel family of divergent seven-transmembrane proteins: candidate odorant receptors in Drosophila. Neuron. 1999;22(2):327-38. PubMed PMID: 10069338.
33. Gao Q, Chess A. Identification of candidate Drosophila olfactory receptors from genomic DNA sequence. Genomics. 1999;60(1):31-9. doi: 10.1006/geno.1999.5894. PubMed PMID: 10458908.
34. Vosshall LB, Amrein H, Morozov PS, Rzhetsky A, Axel R. A spatial map of olfactory receptor expression in the Drosophila antenna. Cell. 1999;96(5):725-36. PubMed PMID: 10089887.
35. Buck L, Axel R. A novel multigene family may encode odorant receptors: a molecular basis for odor recognition. Cell. 1991;65(1):175-87. PubMed PMID: 1840504.
36. Riesgo-Escovar J, Raha D, Carlson JR. Requirement for a phospholipase C in odor response: overlap between olfaction and vision in Drosophila. Proc Natl Acad Sci U S A. 1995;92(7):2864-8. doi: 10.1073/pnas.92.7.2864. PubMed PMID: 7708738; PMCID: PMC42319.
37. Boekhoff I, Strotmann J, Raming K, Tareilus E, Breer H. Odorant-sensitive phospholipase C in insect antennae. Cell Signal. 1990;2(1):49-56. PubMed PMID: 2176800.
38. Breer H, Boekhoff I, Tareilus E. Rapid kinetics of second messenger formation in olfactory transduction. Nature. 1990;345(6270):65-8. doi: 10.1038/345065a0. PubMed PMID: 2158631.
39. Benton R, Sachse S, Michnick SW, Vosshall LB. Atypical membrane topology and heteromeric function of Drosophila odorant receptors in vivo. PLoS Biol. 2006;4(2):e20. doi: 10.1371/journal.pbio.0040020. PubMed PMID: 16402857; PMCID: PMC1334387.
40. Lundin C, Kall L, Kreher SA, Kapp K, Sonnhammer EL, Carlson JR, Heijne G, Nilsson I. Membrane topology of the Drosophila OR83b odorant receptor. FEBS Lett. 2007;581(29):5601-4. doi: 10.1016/j.febslet.2007.11.007. PubMed PMID: 18005664; PMCID: PMC2176074.

41. Larsson MC, Domingos AI, Jones WD, Chiappe ME, Amrein H, Vosshall LB. Or83b encodes a broadly expressed odorant receptor essential for Drosophila olfaction. Neuron. 2004;43(5):703-14. doi: 10.1016/j.neuron.2004.08.019. PubMed PMID: 15339651.
42. Elmore T, Ignell R, Carlson JR, Smith DP. Targeted mutation of a Drosophila odor receptor defines receptor requirement in a novel class of sensillum. J Neurosci. 2003;23(30):9906-12. PubMed PMID: 14586020.
43. Wicher D, Schafer R, Bauernfeind R, Stensmyr MC, Heller R, Heinemann SH, Hansson BS. Drosophila odorant receptors are both ligand-gated and cyclic-nucleotide-activated cation channels. Nature. 2008;452(7190):1007-11. doi: 10.1038/nature06861. PubMed PMID: 18408711.
44. Krieger J, Klink O, Mohl C, Raming K, Breer H. A candidate olfactory receptor subtype highly conserved across different insect orders. J Comp Physiol A Neuroethol Sens Neural Behav Physiol. 2003;189(7):519-26. doi: 10.1007/s00359-003-0427-x. PubMed PMID: 12827420.
45. Jones WD, Nguyen TA, Kloss B, Lee KJ, Vosshall LB. Functional conservation of an insect odorant receptor gene across 250 million years of evolution. Curr Biol. 2005;15(4):R119-21. doi: 10.1016/j.cub.2005.02.007. PubMed PMID: 15723778.
46. Butterwick JA, Del Marmol J, Kim KH, Kahlson MA, Rogow JA, Walz T, Ruta V. Cryo-EM structure of the insect olfactory receptor Orco. Nature. 2018;560(7719):447-52. doi: 10.1038/s41586-018-0420-8. PubMed PMID: 30111839; PMCID: PMC6129982.
47. Sato K, Pellegrino M, Nakagawa T, Nakagawa T, Vosshall LB, Touhara K. Insect olfactory receptors are heteromeric ligand-gated ion channels. Nature. 2008;452(7190):1002-6. doi: 10.1038/nature06850. PubMed PMID: 18408712.
48. Nakagawa T, Pellegrino M, Sato K, Vosshall LB, Touhara K. Amino acid residues contributing to function of the heteromeric insect olfactory receptor complex. PLoS One. 2012;7(3):e32372. doi: 10.1371/journal.pone.0032372. PubMed PMID: 22403649; PMCID: PMC3293798.
49. Guo H, Kunwar K, Smith D. Odorant Receptor Sensitivity Modulation in Drosophila. J Neurosci. 2017;37(39):9465-73. doi: 10.1523/JNEUROSCI.1573-17.2017. PubMed PMID: 28871035; PMCID: PMC5618264.
50. Clyne PJ, Warr CG, Carlson JR. Candidate taste receptors in Drosophila. Science. 2000;287(5459):1830-4. PubMed PMID: 10710312.
51. Scott K, Brady R, Jr., Cravchik A, Morozov P, Rzhetsky A, Zuker C, Axel R. A chemosensory gene family encoding candidate gustatory and olfactory receptors in Drosophila. Cell. 2001;104(5):661-73. PubMed PMID: 11257221.
52. Kwon JY, Dahanukar A, Weiss LA, Carlson JR. The molecular basis of CO2 reception in Drosophila. Proc Natl Acad Sci U S A. 2007;104(9):3574-8. doi: 10.1073/pnas.0700079104. PubMed PMID: 17360684; PMCID: PMC1805529.
53. Jones WD, Cayirlioglu P, Kadow IG, Vosshall LB. Two chemosensory receptors together mediate carbon dioxide detection in Drosophila. Nature. 2007;445(7123):86-90. doi: 10.1038/nature05466. PubMed PMID: 17167414.
54. Gupta BP, Rodrigues V. Atonal is a proneural gene for a subset of olfactory sense organs in Drosophila. Genes Cells. 1997;2(3):225-33. PubMed PMID: 9189759.

55. Abuin L, Bargeton B, Ulbrich MH, Isacoff EY, Kellenberger S, Benton R. Functional architecture of olfactory ionotropic glutamate receptors. Neuron. 2011;69(1):44-60. doi: 10.1016/j.neuron.2010.11.042. PubMed PMID: 21220098; PMCID: PMC3050028.
56. Cao LH, Jing BY, Yang D, Zeng X, Shen Y, Tu Y, Luo DG. Distinct signaling of Drosophila chemoreceptors in olfactory sensory neurons. Proc Natl Acad Sci U S A. 2016;113(7):E902-11. doi: 10.1073/pnas.1518329113. PubMed PMID: 26831094; PMCID: PMC4763727.
57. Benton R, Vannice KS, Vosshall LB. An essential role for a CD36-related receptor in pheromone detection in Drosophila. Nature. 2007;450(7167):289-93. doi: 10.1038/nature06328. PubMed PMID: 17943085.
58. Jin X, Ha TS, Smith DP. SNMP is a signaling component required for pheromone sensitivity in Drosophila. Proc Natl Acad Sci U S A. 2008;105(31):10996-1001. doi: 10.1073/pnas.0803309105. PubMed PMID: 18653762; PMCID: PMC2504837.
59. Li Z, Ni JD, Huang J, Montell C. Requirement for Drosophila SNMP1 for rapid activation and termination of pheromone-induced activity. PLoS Genet. 2014;10(9):e1004600. doi: 10.1371/journal.pgen.1004600. PubMed PMID: 25255106; PMCID: PMC4177743.
60. Gomez-Diaz C, Bargeton B, Abuin L, Bukar N, Reina JH, Bartoi T, Graf M, Ong H, Ulbrich MH, Masson JF, Benton R. A CD36 ectodomain mediates insect pheromone detection via a putative tunnelling mechanism. Nat Commun. 2016;7:11866. doi: 10.1038/ncomms11866. PubMed PMID: 27302750; PMCID: PMC4912623.
61. Neculai D, Schwake M, Ravichandran M, Zunke F, Collins RF, Peters J, Neculai M, Plumb J, Loppnau P, Pizarro JC, Seitova A, Trimble WS, Saftig P, Grinstein S, Dhe-Paganon S. Structure of LIMP-2 provides functional insights with implications for SR-BI and CD36. Nature. 2013;504(7478):172-6. doi: 10.1038/nature12684. PubMed PMID: 24162852.
62. Wachowiak M. Active Sensing in Olfaction. In: Menini A, editor. The Neurobiology of Olfaction. Boca Raton (FL)2010.
63. Kalidas S, Smith DP. Novel genomic cDNA hybrids produce effective RNA interference in adult Drosophila. Neuron. 2002;33(2):177-84. PubMed PMID: 11804566.
64. Ignatious Raja JS, Katanayeva N, Katanaev VL, Galizia CG. Role of Go/i subgroup of G proteins in olfactory signaling of Drosophila melanogaster. Eur J Neurosci. 2014;39(8):1245-55. doi: 10.1111/ejn.12481. PubMed PMID: 24443946; PMCID: PMC4324130.
65. Talluri S, Bhatt A, Smith DP. Identification of a Drosophila G protein alpha subunit (dGq alpha-3) expressed in chemosensory cells and central neurons. Proc Natl Acad Sci U S A. 1995;92(25):11475-9. doi: 10.1073/pnas.92.25.11475. PubMed PMID: 8524786; PMCID: PMC40424.
66. Deng Y, Zhang W, Farhat K, Oberland S, Gisselmann G, Neuhaus EM. The stimulatory Galpha(s) protein is involved in olfactory signal transduction in Drosophila. PLoS One. 2011;6(4):e18605. doi: 10.1371/journal.pone.0018605. PubMed PMID: 21490930; PMCID: PMC3072409.
67. Vogt RG, Riddiford LM. Pheromone binding and inactivation by moth antennae. Nature. 1981;293(5828):161-3. PubMed PMID: 18074618.
68. Steinbrecht RA, Ozaki M., Ziegelberger, G. Immunocytochemical localization of pheromone-binding protein in moth antennae. Cell Tissue Res. 1992;270:287-302.

69. Klein U. Sensillum-lymph proteins from antennal olfactory hairs of the moth Antheraea polyphemus (Saturniidae). Insect Biochemistry. 1987;17(8):1193-204. doi: https://doi.org/10.1016/0020-1790(87)90093-X.
70. P. Pelosi RM. Odorant binding proteins in vertebrates and insects: similarities and possible common function. Chem Senses. 1990;15(2):205-15. doi: https://doi.org/10.1093/chemse/15.2.205.
71. Vogt RG, Prestwich GD, Lerner MR. Odorant-binding-protein subfamilies associate with distinct classes of olfactory receptor neurons in insects. J Neurobiol. 1991;22(1):74-84. doi: 10.1002/neu.480220108. PubMed PMID: 2010751.
72. Breer H, Krieger, J,. Raming K. A novel class of binding proteins in the antennae of the silk moth Antheraea pernyi. Insect Biochemistry. 1990;20(7):735-40.
73. Zhou JJ, Huang W, Zhang GA, Pickett JA, Field LM. "Plus-C" odorant-binding protein genes in two Drosophila species and the malaria mosquito Anopheles gambiae. Gene. 2004;327(1):117-29. doi: 10.1016/j.gene.2003.11.007. PubMed PMID: 14960367.
74. Vieira FG, Rozas J. Comparative genomics of the odorant-binding and chemosensory protein gene families across the Arthropoda: origin and evolutionary history of the chemosensory system. Genome Biol Evol. 2011;3:476-90. doi: 10.1093/gbe/evr033. PubMed PMID: 21527792; PMCID: PMC3134979.
75. Sandler BH, Nikonova L, Leal WS, Clardy J. Sexual attraction in the silkworm moth: structure of the pheromone-binding-protein-bombykol complex. Chem Biol. 2000;7(2):143-51. PubMed PMID: 10662696.
76. Vogt RG, Riddiford LM, Prestwich GD. Kinetic properties of a sex pheromone-degrading enzyme: the sensillar esterase of Antheraea polyphemus. Proc Natl Acad Sci U S A. 1985;82(24):8827-31. doi: 10.1073/pnas.82.24.8827. PubMed PMID: 3001718; PMCID: PMC391531.
77. van der Goot FG, Gonzalez-Manas JM, Lakey JH, Pattus F. A 'molten-globule' membrane-insertion intermediate of the pore-forming domain of colicin A. Nature. 1991;354(6352):408-10. doi: 10.1038/354408a0. PubMed PMID: 1956406.
78. Wojtasek H, Leal WS. Conformational change in the pheromone-binding protein from Bombyx mori induced by pH and by interaction with membranes. J Biol Chem. 1999;274(43):30950-6. PubMed PMID: 10521490.
79. Kaissling KE. Peripheral mechanisms of pheromone reception in moths. Chem Senses. 1996;21(2):257-68. doi: 10.1093/chemse/21.2.257. PubMed PMID: 8670704.
80. Ziegelberger G. Redox-shift of the pheromone-binding protein in the silkmoth Antheraea polyphemus. Eur J Biochem. 1995;232(3):706-11. PubMed PMID: 7588707.
81. Kim MS, Repp A, Smith DP. LUSH odorant-binding protein mediates chemosensory responses to alcohols in Drosophila melanogaster. Genetics. 1998;150(2):711-21. PubMed PMID: 9755202; PMCID: PMC1460366.
82. Shanbhag SR, Hekmat-Scafe D, Kim MS, Park SK, Carlson JR, Pikielny C, Smith DP, Steinbrecht RA. Expression mosaic of odorant-binding proteins in Drosophila olfactory organs. Microsc Res Tech. 2001;55(5):297-306. doi: 10.1002/jemt.1179. PubMed PMID: 11754509.

83. Kruse SW, Zhao R, Smith DP, Jones DN. Structure of a specific alcohol-binding site defined by the odorant binding protein LUSH from Drosophila melanogaster. Nat Struct Biol. 2003;10(9):694-700. doi: 10.1038/nsb960. PubMed PMID: 12881720; PMCID: PMC4397894.
84. Laughlin JD, Ha TS, Jones DNM, Smith DP. Activation of pheromone-sensitive neurons is mediated by conformational activation of pheromone-binding protein. Cell. 2008;133(7):1255-65. doi: 10.1016/j.cell.2008.04.046. PubMed PMID: 18585358; PMCID: PMC4397981.
85. Ronderos DS, Smith DP. Activation of the T1 neuronal circuit is necessary and sufficient to induce sexually dimorphic mating behavior in Drosophila melanogaster. J Neurosci. 2010;30(7):2595-9. doi: 10.1523/JNEUROSCI.4819-09.2010. PubMed PMID: 20164344; PMCID: PMC3426441.
86. Gomez-Diaz C, Reina JH, Cambillau C, Benton R. Ligands for pheromone-sensing neurons are not conformationally activated odorant binding proteins. PLoS Biol. 2013;11(4):e1001546. doi: 10.1371/journal.pbio.1001546. PubMed PMID: 23637570; PMCID: PMC3640100.
87. Galindo K, Smith DP. A large family of divergent Drosophila odorant-binding proteins expressed in gustatory and olfactory sensilla. Genetics. 2001;159(3):1059-72. PubMed PMID: 11729153; PMCID: PMC1461854.
88. Hekmat-Scafe DS, Dorit RL, Carlson JR. Molecular evolution of odorant-binding protein genes OS-E and OS-F in Drosophila. Genetics. 2000;155(1):117-27. PubMed PMID: 10790388; PMCID: PMC1461081.
89. Larter NK, Sun JS, Carlson JR. Organization and function of Drosophila odorant binding proteins. Elife. 2016;5. doi: 10.7554/eLife.20242. PubMed PMID: 27845621; PMCID: PMC5127637.
90. Swarup S, Williams TI, Anholt RR. Functional dissection of Odorant binding protein genes in Drosophila melanogaster. Genes Brain Behav. 2011;10(6):648-57. doi: 10.1111/j.1601-183X.2011.00704.x. PubMed PMID: 21605338; PMCID: PMC3150612.
91. Swarup S, Morozova TV, Sridhar S, Nokes M, Anholt RR. Modulation of feeding behavior by odorant-binding proteins in Drosophila melanogaster. Chem Senses. 2014;39(2):125-32. doi: 10.1093/chemse/bjt061. PubMed PMID: 24302688; PMCID: PMC3894858.
92. Jeong YT, Shim J, Oh SR, Yoon HI, Kim CH, Moon SJ, Montell C. An odorant-binding protein required for suppression of sweet taste by bitter chemicals. Neuron. 2013;79(4):725-37. doi: 10.1016/j.neuron.2013.06.025. PubMed PMID: 23972598; PMCID: PMC3753695.
93. Knecht ZA, Silbering AF, Cruz J, Yang L, Croset V, Benton R, Garrity PA. Ionotropic Receptor-dependent moist and dry cells control hygrosensation in Drosophila. Elife. 2017;6. doi: 10.7554/eLife.26654. PubMed PMID: 28621663; PMCID: PMC5495567.
94. Shanbhag SR, Singh K, Singh RN. Fine structure and primary sensory projections of sensilla located in the sacculus of the antenna of Drosophila melanogaster. Cell Tissue Res. 1995;282(2):237-49. PubMed PMID: 8565054.
95. Sun JS, Larter NK, Chahda JS, Rioux D, Gumaste A, Carlson JR. Humidity response depends on the small soluble protein Obp59a in Drosophila. Elife. 2018;7. doi: 10.7554/eLife.39249. PubMed PMID: 30230472; PMCID: PMC6191283.

96. McKenna MP, Hekmat-Scafe DS, Gaines P, Carlson JR. Putative Drosophila pheromone-binding proteins expressed in a subregion of the olfactory system. J Biol Chem. 1994;269(23):16340-7. PubMed PMID: 8206941.
97. Hekmat-Scafe DS, Steinbrecht RA, Carlson JR. Coexpression of two odorant-binding protein homologs in Drosophila: implications for olfactory coding. J Neurosci. 1997;17(5):1616-24. PubMed PMID: 9030621.
98. Bentzur A, Shmueli A, Omesi L, Ryvkin J, Knapp JM, Parnas M, Davis FP, Shohat-Ophir G. Odorant binding protein 69a connects social interaction to modulation of social responsiveness in Drosophila. PLoS Genet. 2018;14(4):e1007328. doi: 10.1371/journal.pgen.1007328. PubMed PMID: 29630598; PMCID: PMC5908198.
99. Vieira FG, Sanchez-Gracia A, Rozas J. Comparative genomic analysis of the odorant-binding protein family in 12 Drosophila genomes: purifying selection and birth-and-death evolution. Genome Biol. 2007;8(11):R235. doi: 10.1186/gb-2007-8-11-r235. PubMed PMID: 18039354; PMCID: PMC2258175.
100. Kondo S, Ueda R. Highly improved gene targeting by germline-specific Cas9 expression in Drosophila. Genetics. 2013;195(3):715-21. doi: 10.1534/genetics.113.156737. PubMed PMID: 24002648; PMCID: PMC3813859.
101. Wang L, Han X, Mehren J, Hiroi M, Billeter JC, Miyamoto T, Amrein H, Levine JD, Anderson DJ. Hierarchical chemosensory regulation of male-male social interactions in Drosophila. Nat Neurosci. 2011;14(6):757-62. doi: 10.1038/nn.2800. PubMed PMID: 21516101; PMCID: PMC3102769.
102. Gratz SJ, Ukken FP, Rubinstein CD, Thiede G, Donohue LK, Cummings AM, O'Connor-Giles KM. Highly specific and efficient CRISPR/Cas9-catalyzed homology-directed repair in Drosophila. Genetics. 2014;196(4):961-71. doi: 10.1534/genetics.113.160713. PubMed PMID: 24478335; PMCID: PMC3982687.
103. Pirrotta V. Vectors for P-mediated transformation in Drosophila. Biotechnology. 1988;10:437-56. PubMed PMID: 2850048.
104. Rubin GM, Spradling AC. Genetic transformation of Drosophila with transposable element vectors. Science. 1982;218(4570):348-53. PubMed PMID: 6289436.
105. Nandi N, Tyra LK, Stenesen D, Kramer H. Stress-induced Cdk5 activity enhances cytoprotective basal autophagy in Drosophila melanogaster by phosphorylating acinus at serine(437). Elife. 2017;6. doi: 10.7554/eLife.30760. PubMed PMID: 29227247; PMCID: PMC5760206.
.